

December 2016

Sedimentology of Pleistocene Outwash and Glaciolacustrine Deposits in East-central Wisconsin

Carrie Czech

University of Wisconsin-Milwaukee

Follow this and additional works at: <https://dc.uwm.edu/etd>



Part of the [Geology Commons](#)

Recommended Citation

Czech, Carrie, "Sedimentology of Pleistocene Outwash and Glaciolacustrine Deposits in East-central Wisconsin" (2016). *Theses and Dissertations*. 1357.

<https://dc.uwm.edu/etd/1357>

This Thesis is brought to you for free and open access by UWM Digital Commons. It has been accepted for inclusion in Theses and Dissertations by an authorized administrator of UWM Digital Commons. For more information, please contact open-access@uwm.edu.

SEDIMENTOLOGY OF PLEISTOCENE
OUTWASH AND GLACIOLACUSTRINE DEPOSITS
IN EAST-CENTRAL WISCONSIN

by

Carrie Czech

A Thesis Submitted in
Partial Fulfillment of the
Requirements for the Degree of

Master of Science
in Geosciences

at

The University of Wisconsin-Milwaukee

December 2016

ABSTRACT

SEDIMENTOLOGY OF PLEISTOCENE OUTWASH AND GLACIOLACUSTRINE DEPOSITS IN EAST-CENTRAL WISCONSIN

by

Carrie Czech

The University of Wisconsin-Milwaukee, 2016
Under the Supervision of Professor John Isbell

The Green Bay Lobe was one of several lobes of the Laurentide Ice Sheet (LIS) to enter Wisconsin during the recent Wisconsinan glaciation. Kewaunee Formation deposits in the Tower Hill sand and gravel pit near the city of De Pere in east-central Wisconsin were previously interpreted to be the result of an ice-contact delta, prograding into former glacial Lake Oshkosh (Mickelson and Mode, 2007). Estimates of water depth in the lake had been poorly constrained as they had been estimated by the elevation of the outlet channels and a few scattered, poorly-preserved strandline deposits (Hooyer, 2007). Reexamination of these Kewaunee Formation deposits suggests they were part of a grounding-line fan system prograding into glacial Lake Oshkosh, that glacial Lake Oshkosh was an ice-contact lake with a dynamic ice front, and that lake levels changed throughout time. The occurrence of wave ripples found as basal deposits in most sections suggests that water depth, although not measurable, was relatively shallow with at least one large draining event. Thrust sheets in silt, superimposed styles of different types of folding, and different orientations of sediment rafts, nappe-like structures, and/or sheath(-like) folds suggests deformation that occurred in the northwest corner of the pit was by ice shove with a nearby ice margin (Mills and Wells, 1974). By addressing the aforementioned topics, the

ice dynamics (i.e., ice recession and readvance history) of the Green Bay Lobe during deposition of the Kewaunee Formation has been more fully resolved.

© Copyright by Carrie Czech, 2016
All Rights Reserved

In loving memory of my grandparents,

John & Josephine,

my first and best teachers

TABLE OF CONTENTS

Abstract.....	ii
List of Figures.....	viii
Acknowledgements.....	xii
CHAPTER	PAGE
1 INTRODUCTION.....	1
2 METHODS.....	11
3 FACIES.....	14
3.1 Deformed Sand Facies.....	14
3.1.1 Description.....	14
3.1.2 Interpretation.....	16
3.2 Symmetrical-Rippled Facies.....	17
3.2.1 Description.....	17
3.2.2 Interpretation.....	23
3.3 Unidirectional Bedform Facies Assemblages.....	24
3.3.1 Description.....	24
3.3.1a Cross-bedded Sand with Faulting Description.....	29
3.3.2 Interpretation.....	31
3.3.2a Cross-bedded Sand with Faulting Interpretation....	32
3.4 Gravel Facies.....	33
3.4.1 Description.....	33
3.4.2 Interpretation.....	36
3.5 Deformed Facies.....	37
3.5.1 Description.....	37
3.5.2 Interpretation.....	43
3.6 Diamict Facies.....	45
3.6.1 Description.....	45
3.6.2 Interpretation.....	46
4 ENVIRONMENTAL DISCUSSION.....	46
5 CONCLUSIONS.....	54
6 REFERENCES.....	55
7 APPENDICES.....	59
Appendix A: Paleocurrent Measurements.....	59
Appendix B: Key to be Referenced for all Stratigraphic Columns.....	60
Appendix C: Author’s Complete Stratigraphic Columns.....	61

Appendix D: List of Abbreviations to be used with Stratigraphic Columns.....	81
Appendix E: Electrical profile data generated using an ARES Resistivity System...	82

LIST OF FIGURES

Figure 1. Maps depicting changes in Laurentide Ice Sheet coverage over Wisconsin from 31,000 – 13,250 y.b.p. with extent of glacial ice coverage of the Green Bay Lobe. Orange star represents field site and glacial ice coverage conditions through time. Modified from Syverson et al. (2011).....	2
Figure 2. Deposits of the various lobes of the Laurentide Ice Sheet in Wisconsin. Field study area is highlighted with orange boxes and associated time period of interest falls between orange dashed lines. Modified from Syverson et al. (2011).....	3
Figure 3. Map depicting the four main drainage outlets associated with the Green Bay Lobe and their corresponding elevations. From Hooyer (2007).....	5
Figure 4. Lithostratigraphic units, glacial phases, lake stages, lake outlets, lake levels, and corresponding dates of glacial Lake Oshkosh. Area between orange dashed lines represents time period of interest. Modified from Hooyer (2007).....	6
Figure 5. (A) Map of the Pleistocene Geology of Brown County, Wisconsin; (B) Associated map legend. Orange stars represent field site and associated geology. Modified from Need (1983).....	7
Figure 6. Part of U.S. Geological Survey De Pere Quadrangle, 1971. Location of Tower Hill sand and gravel pit field site is approximately N44°24', W88°00' and denoted by orange star. Modified from Mickelson and Mode (2007).....	9
Figure 7. Reconstructed stratigraphy of the Tower Hill sand and gravel pit with interpretation by Mickelson and Mode (2007). Modified from Mickelson and Mode (2007).....	10
Figure 8. (A) Photograph of field site location; (B) Previous photograph with pins marking the locations of stratigraphic sections. Images courtesy of Google Earth. Date of imagery: 03/2010.....	13
Figure 9. (A) Photograph of deformed sand in section VS-4. Hand lens for scale; (B) Previous photograph with deformation structures highlighted.....	15
Figure 10. Photograph of deformed sand.....	16
Figure 11. (A) Photograph of climbing symmetrical ripples occurring beneath red clay layer in section VS-1. Yellow horizontal markings in Jacob's staff are 0.1 m apart; (B) Previous photograph with symmetrical ripples highlighted.....	18
Figure 12. Photograph of symmetrical ripples overlain by cross-bedded sand in section VS-2. Field notebook (7.5 cm in length) for scale.....	19

Figure 13. Photograph of alternating symmetrical and climbing ripples in section VS-3. Pen for scale.....	20
Figure 14. Photograph of alternating symmetrical and climbing ripples in section VS-3. Note rounded ripple crests. Trowel for scale.....	21
Figure 15. Photograph of symmetrical-rippled sand in section VS-1.....	22
Figure 16. Photograph of red clay clasts occurring with Symmetrical-Rippled Facies deposits in section VS-1. Numbers on ruler are 1 cm apart; entire ruler is 30 cm in length.....	23
Figure 17. Photograph of cross-bedding in sand in section VS-2. Flow direction was from left to right. Brunton compass for scale. Note slight angle of climb and downclimbing or downstream accretion to the right of the staff.....	26
Figure 18. Photograph of overturned cross-beds (white arrow) at the top of section VS-8. Thickness of bed is approximately 1 m. Flow direction at the time of overturning was from left to right.....	27
Figure 19. Photograph of a macroform (bar) made of downclimbing ripples.....	28
Figure 20. Photograph of downstream-accreting macroforms with a low angle of climb to the left (west).....	29
Figure 21. (A) Photograph of normal and reverse faults in cross-bedded sand. Jacob's staff for scale; (B) Previous photograph with normal faults (green) and reverse faults (red) highlighted.....	30
Figure 22. Photograph of faulting in sand in an area between sections VS-9 and VS-10..	30
Figure 23. Photograph of reverse faulting in sand between sections VS-9 and VS-10. Trowel for scale.....	31
Figure 24. Photograph of Gravel Facies (containing sections VS-7, VS-8, and VS-9 from right to left). Backpack in lower right corner for scale.....	34
Figure 25. Photograph of gravel dipping upstream. Tape measure placed for measurement of section VS-8. Entire section measures 6.2 m in height. Backpacks for scale.....	34
Figure 26. Photograph of cross-bedded gravel in section VS-8. Entire section measures 6.2 m in height.....	35
Figure 27. Photograph of cross-bedding in gravel in section VS-8. Jacob's staff for scale.....	36

Figure 28. (A) Photograph of the deformed area in 1997. Photograph provided by Dr. William Mode. Truck for scale; (B) Previous photograph with truncation surfaces 1 and 2 annotated.....	38
Figure 29. Photograph of steep steps on truncation surface. Geologist for scale.....	39
Figure 30. Photograph of sand blocks exposed in 1997. Photograph provided by Dr. William Mode. Geologist for scale.....	39
Figure 31. Photograph of sand blocks in gravel.....	40
Figure 32. Photograph of main area of deformation between sections VS-9 and VS-10. Geologist for scale.....	41
Figure 33. Photograph of area near section VS-10 with an overturned front, sheath-fold, and nappe-like block.....	41
Figure 34. Photograph of folding in sand and gravel between sections VS-9 and VS-10..	42
Figure 35. Photograph of diamict overlying sand and gravel in an area between sections VS-9 and VS-10.....	46
Figure 36. Photographs and associated ground penetrating radar (GPR) data of the Tower Hill sand and gravel pit collected by Dr. William Kean in 2010. View is towards the north-northeast. Geologists for scale. See Appendix E for additional metadata.....	48
Figure 37. GPR profile on upper terrace of the Tower Hill sand and gravel pit to 6 m depth collected by Dr. William Kean in 2010. See Appendix E for additional metadata.....	48
Figure 38. Schematic cross sections of interpretation of deposition and lake/glacial dynamics occurring over time: (A) Initial grounding-line fan-building phase; (B) base level fall and formation of truncation surface 1; and (C) ice shove.....	51
Figure 39. Photograph of section VS-1. Orange ruler for scale; entire ruler is 30 cm in length.....	61
Figure 40. Photograph of section VS-2. Field notebook (7.5 cm in length) for scale.....	63
Figure 41. Photograph of section VS-3. Jacob’s staff for scale; yellow lines are 10 cm apart.....	65
Figure 42. Photograph of section VS-4. Jacob’s staff for scale; staff is approximately 1.5 m in length.....	67

Figure 43. Photograph of section VS-5. Entire section measures 6.0 m in height..... 69

Figure 44. Photograph of section VS-6. Entire section measures 6.0 m in height..... 71

Figure 45. Photograph of section VS-7. Jacob’s staff for scale; entire staff is approximately 1.5 m in length..... 73

Figure 46. Photograph of section VS-8. Jacob’s staff for scale; staff is approximately 1.5 m in length..... 75

Figure 47. Photograph of section VS-9. Jacob’s staff for scale; staff is approximately 1.5 m in length..... 77

Figure 48. Photograph of section VS-10..... 79

ACKNOWLEDGEMENTS

First and foremost, I would like to thank Dr. John Isbell for accepting me as a graduate student and his guidance. John, I learned how to be a better scientist, teacher, and person by watching you lead by example these past “couple” of years. Thank you for believing in me. And for reminding me to wear sunscreen while in the field.

I am grateful to the late Dr. Thomas Hooyer for making glacial geology interesting and orienting me to what would later become my thesis field site. Tom, I remember your enthusiasm as you first handed me a piece of the Two Creeks. You will be missed.

Thanks to Dr. Dyanna Czeck and Dr. William Kean for agreeing to serve on my thesis committee. I would like to acknowledge Dr. Kean, along with Dr. David Hart of the Wisconsin Geological and Natural History Survey (WGNHS), for sharing their ground penetrating radar (GPR) data. Dr. Kean, I additionally would like to thank you for sharing your electrical resistivity data.

To the Van Straten family: thank you for allowing land access to your property. This project would not have been possible without you.

Thanks to the following for their assistance in the field: Dr. Ashley Dineen, Zelenda Koch, Susan Krans, Jenny Ulbricht, and Wes Weichert. Thanks to Dr. William Mode for his assistance in the field and providing photographs from earlier field excursions. Dr. J. Elmo Rawling III, thank you for the geology discussions and for pointing me in the direction of additional resources.

I would like to express my gratitude for the generous support of the University of Wisconsin – Milwaukee Geosciences Department. Dr. Theresa (Teri) Boundy, I have the life

experiences I do today because of the doors you helped me open. Thank you for making me feel as though I belonged. Brett Ketter, thank you for the CoreIDRAW and PowerPoint lessons. They were put to good use.

Dr. Glen Fredlund, I did not forget your words of encouragement. Thank you for reminding me to “just keep swimming.”

Daniel Bialzik and Laura Pope, thank you for the consistency of your friendship. I am grateful our paths crossed all of those years ago. Ranger Kathleen (Kathy) Denton, thank you for serving as a mentor to me and being the first to teach me about safety in the field. Nicholas Puetzer and Nathan Winkler, thank you for being open to learning more about my thesis topic and proofreading my drafts. Finally, heartfelt thanks to my remaining family members and friends, too many to mention here by name, who kept encouraging me along the way.

1 INTRODUCTION

The Green Bay Lobe was one of numerous lobes to enter Wisconsin as part of the Laurentide Ice Sheet (LIS) during the recent Wisconsinan glaciations (Figure 1). The last glacial maximum (LGM) occurred approximately 18,500 y.b.p. (Attig et al., 2011), when the Green Bay Lobe extended as far south as Madison and Janesville, Wisconsin, terminating in the Johnstown moraine.

A substantial effort has been made to reconstruct the dynamic advance and recession history of the Green Bay Lobe by: Thwaites and Bertrand (1957), Black (1970), Black (1980), McCartney and Mickelson (1982), Peterson (1986), Mode (1989), Clark (1992), Kaiser (1994), Maher and Mickelson (1996), Colgan and Mickelson (1997), Socha et al. (1999), Cutler et al. (2002), Winguth et al. (2004), Mickelson et al. (2007), Clark et al. (2008), and Hooyer et al. (2009), as well as numerous other authors. As the Green Bay Lobe entered the Fox River Valley, the northward surface water drainage route of the ancestral Fox River became obstructed, allowing the formation of glacial Lake Oshkosh. A total of 3 advance-recession cycles have been identified in the last 30,000 years, with a total of five different related expansion-contraction cycles of this lake (Hooyer, 2007; Syverson et al., 2011).

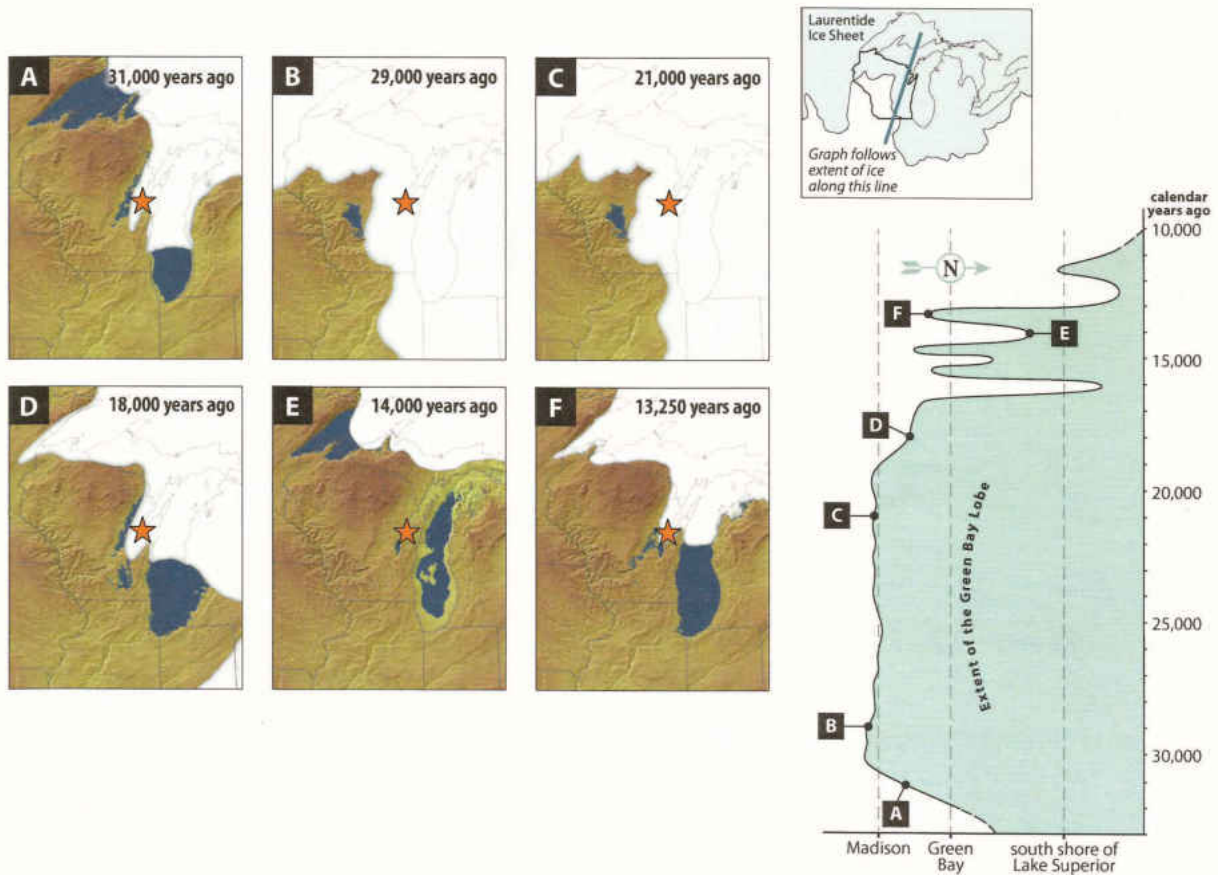


Figure 1. Maps depicting changes in Laurentide Ice Sheet coverage over Wisconsin from 31,000 – 13,250 y.b.p. (left) with extent of glacial ice coverage of the Green Bay Lobe (right). Orange star represents field site and glacial ice coverage conditions through time. Modified from Syverson et al. (2011).

Glacial Lake Oshkosh has been interpreted to have been an ice-contact, proglacial lake (Mickelson and Mode, 2007) that persisted in some form until the Green Bay Lobe receded northward out of Wisconsin, and the lake drained into the Lake Michigan Basin through a series of channels cut into a southwestward extending Silurian escarpment that separated the Green Bay Lobe from the Lake Michigan Lobe (Hooyer, 2007). Recession of the Green Bay Lobe stemmed from a greater waning of the LIS glaciation in the Midwest United States, which progressed into long-term glacial recession.

Ice dynamics along the margin of the Green Bay Lobe during deposition of the Kewaunee Formation are poorly understood, as is the relationship between the ice front and glacial Lake Oshkosh. Although the elevation and water depth of glacial Lake Oshkosh are assumed to have been controlled by the location of the ice margin and the elevation of the outlet channels cut into the Silurian escarpment (Figure 3), it is unknown whether glacial ice was in contact with lake waters or was separated by an outwash plain. Estimates of water depth in the lake are also poorly constrained (Figure 4) as they are currently estimated by the elevation of the outlet channels, and a few scattered, poorly-preserved strandline deposits (Hooyer, 2007). Additional lines of evidence are required to more accurately estimate water depths in glacial Lake Oshkosh. This paper explores the dynamics of glacial Lake Oshkosh-ice front interactions with focus on Green Bay Lobe deposits in the Tower Hill sand and gravel pit in Brown County (Figure 5) near De Pere, Wisconsin (Figure 6) in the interval between deposition of the Chilton and Glenmore tills of the Kewaunee Formation (Figure 7). At this site, sand and gravel that prograded into glacial Lake Oshkosh are overlain by strata equivalent to the Two Creeks forest bed and the Glenmore diamict. Therefore, this site contains a record of ice-lake interactions during recession of the Chilton Member and advance of the Glenmore Member.

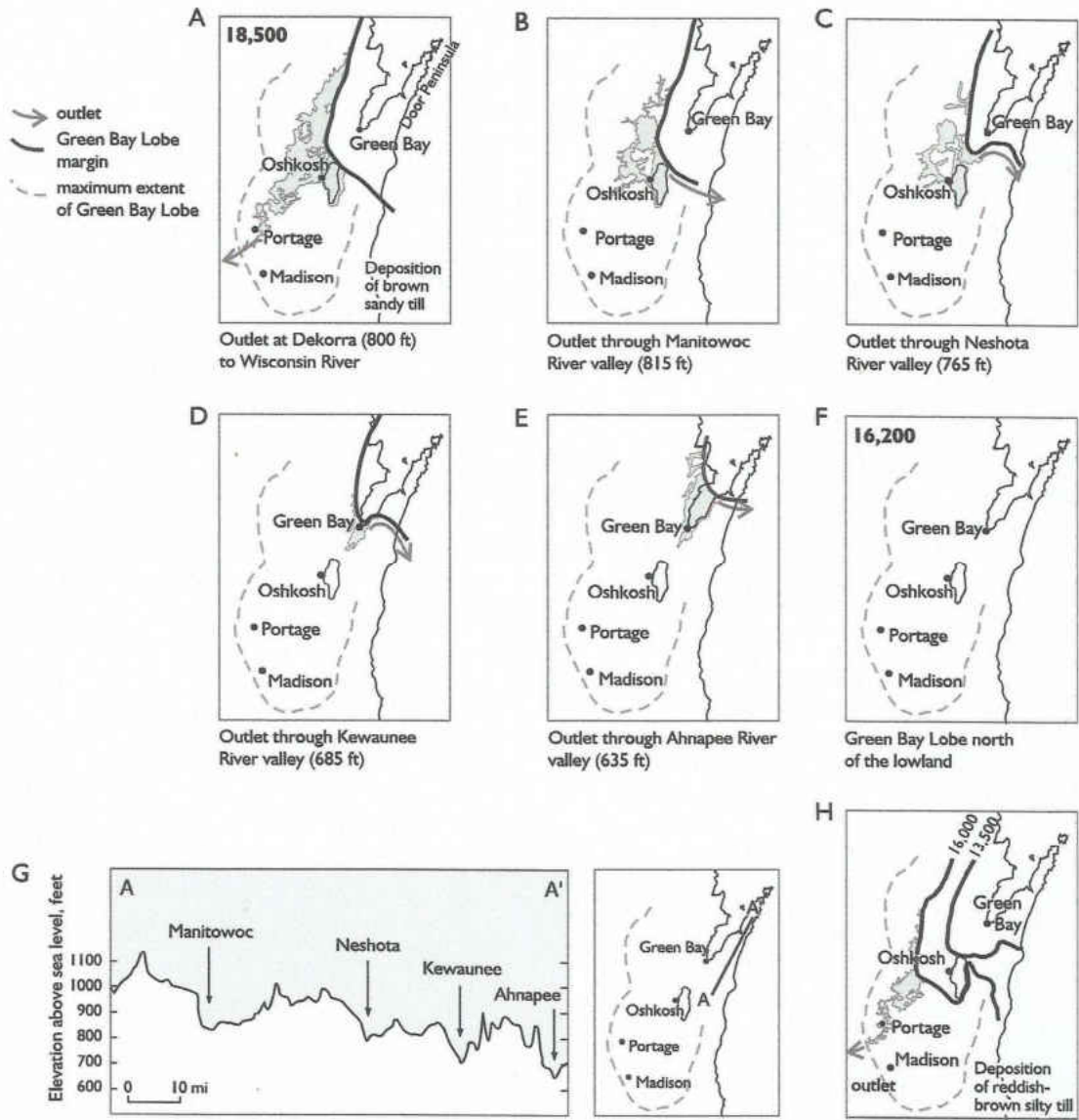


Figure 3. Map depicting the four main drainage outlets associated with the Green Bay Lobe and their corresponding elevations. From Hooyer (2007).

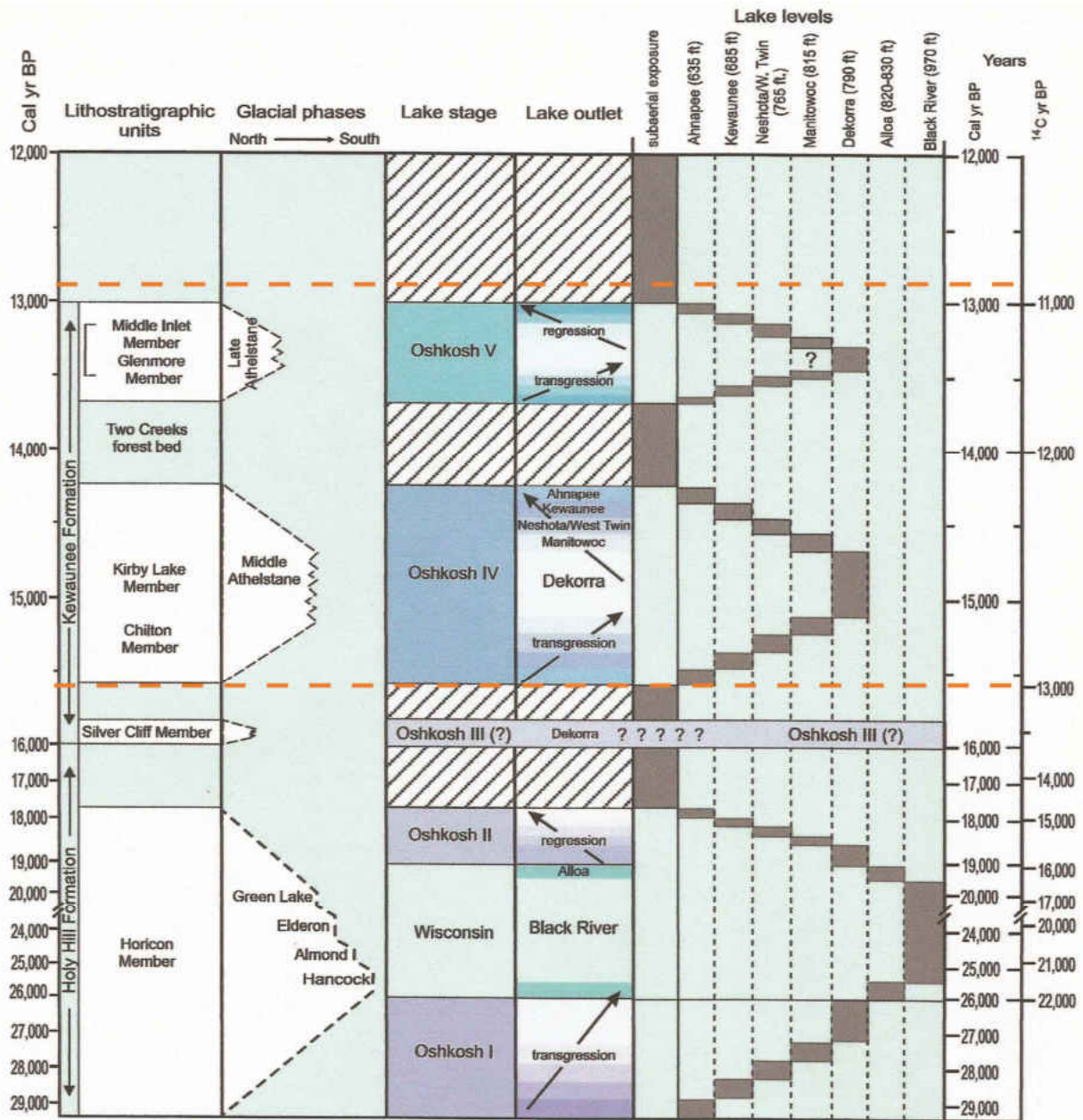


Figure 4. Lithostratigraphic units, glacial phases, lake stages, lake outlets, lake levels, and corresponding dates of glacial Lake Oshkosh. Area between orange dashed lines represents time period of interest. Modified from Hooyer (2007).

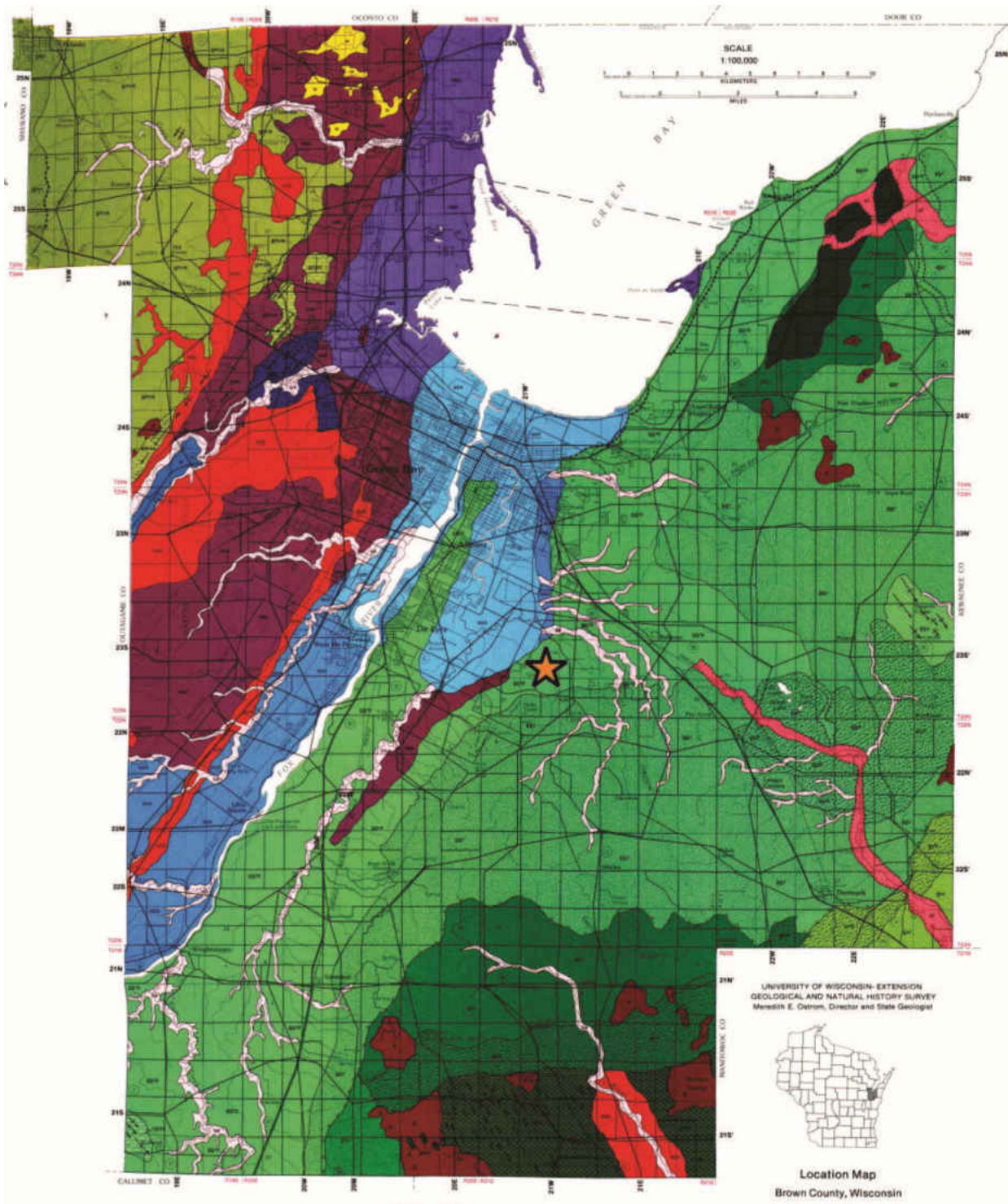




Figure 5. (A) Map of the Pleistocene Geology of Brown County, Wisconsin; (B) Associated map legend. Orange stars represent field site and associated geology. Modified from Need (1983).

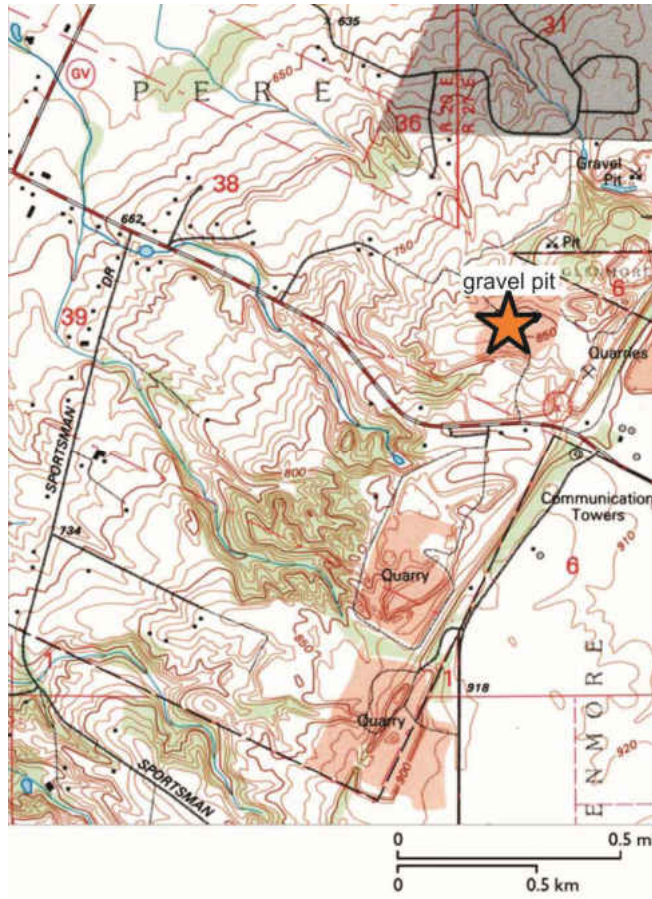


Figure 6. Part of U.S. Geological Survey De Pere Quadrangle, 1971. Location of Tower Hill sand and gravel pit field site is approximately $N44^{\circ}24'$, $W88^{\circ}00'$ and denoted by orange star. Modified from Mickelson and Mode (2007).

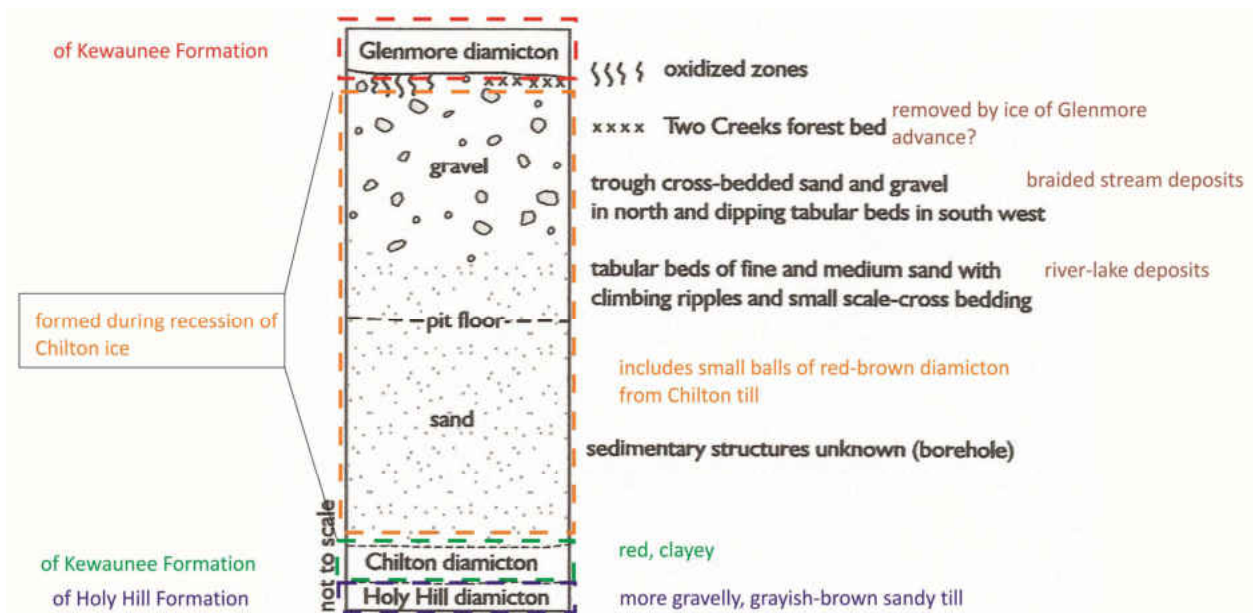


Figure 7. Reconstructed stratigraphy of the Tower Hill sand and gravel pit with interpretation by Mickelson and Mode (2007). Modified from Mickelson and Mode (2007).

To better understand ice and lake dynamics following deposition of the Chilton diamicton and associated ice readvance during deposition of the Glenmore diamicton, a number of questions can be addressed by investigating strata in the Tower Hill sand and gravel pit. These include questions discussed below.

1.) Are deposits of glacial Lake Oshkosh preserved in the Tower Hill sand and gravel pit?

Were the sand and gravel deposits in the Tower Hill gravel pit a Gilbert-like delta (deposits containing bottomset beds, steeply-dipping foreset beds, and topset beds), a grounding-line fan, or some other geomorphic element? Mickelson and Mode (2007) interpreted the Tower Hill gravel pit as a prograding delta along the eastern edge of glacial Lake Oshkosh. If this interpretation is correct, the height of the Gilbert delta would constrain the elevation of glacial Lake Oshkosh. If it was a grounding-line fan, the sand and gravel would have been deposited subaqueously and would not necessarily

provide an estimate of water depth (Powell, 1990). Mickelson and Mode (2007) suggested that a delta occurred in the southwestern portion of the original pit, while braided stream deposits occurred in the northeastern portion of the pit.

- 2.) What was the water depth in the area of the Tower Hill gravel pit when the sand and gravel were being deposited? Water depths only can be estimated if deposits of a Gilbert delta are present or if the deposits are that of a grounding-line fan that grew into a subaerial delta.
- 3.) Where was the ice in relation to glacial Lake Oshkosh? Was glacial Lake Oshkosh indeed an ice-contact lake or was the ice separated from the lake by an outwash plain as Mickelson and Mode (2007) suggested.
- 4.) A final question warranting further exploration relates to deformation that occurs towards the northwest corner of the gravel pit. Was this deformation due to: (1) slumping, (2) ice shove, or (3) loading and rapid sedimentation (from hydrofracturing which would have a rupture-like structure)? Slumping or collapse could suggest stagnant ice. Slumping could also suggest progradation of sediment, whereas ice shove would suggest glacial readvance.

By addressing the aforementioned questions, the ice readvance and recession history of the Green Bay Lobe during deposition of the Kewaunee Formation can be more fully resolved.

2 METHODS

Six days, between August of 2009 and September of 2011, were spent conducting fieldwork in the Tower Hill sand and gravel pit located in Brown County, Wisconsin. Land access permission was granted by the Van Straten family. The gravel pit was, and likely still is, an active

quarry from which sand and gravel were being mined. As such, exposures were continuously changing over time. The field site was examined and photographed to investigate the overall sediment facies, geometries of beds, and sequence stratigraphy. A Jacob's staff and Abney level were used to measure ten stratigraphic sections (Figure 8). A handheld Global Position System (GPS) unit was utilized to denote the location of each section. For sections that could not be accessed by measuring upwards, a measuring tape was lowered from an upper surface to measure from the top downwards. Bounding surfaces, contacts, sediment composition/grain size, and sedimentary structures were measured, described, and photographed. A grain-size comparator was used to identify sediment size using the Wentworth classification system. A Brunton compass was used to measure paleocurrent orientations of asymmetrical ripples (Appendix A). Orientation data were subjected to circular statistical methods using Rick Allmendinger's Stereonet 9 (Allmendinger, 2016) (Appendix A) to calculate a vector length which represents the degree to which data (i.e., paleocurrents) cluster, with a higher vector length value representing data with less deviation from the mean. Stratigraphic columns were drafted using CorelDraw. These columns were then used to summarize the sedimentology of the succession within the sand and gravel pit. Ground penetrating radar (GPR) data (see 4 Environmental Discussion, Figures 36 and 37; Appendix E), and electrical profile data (see Appendix E) were obtained and shared by Dr. William Kean of the University of Wisconsin – Milwaukee and Dr. David Hart of the Wisconsin Geological and Natural History Survey.



Figure 8. (A) (top) Photograph of field site location; (B) (bottom) Previous photograph with pins marking the locations of stratigraphic sections. Images courtesy of Google Earth. Date of imagery: 03/2010.

Sections VS-1, VS-2, VS-3, VS-4, VS-5, and VS-6 are comprised mostly of unconsolidated sand. Unconsolidated gravel occurs in sections VS-7, VS-8, and VS-9. Deformed strata occur in an area between sections VS-9 and VS-10. Facies here are introduced in the order in which they were measured in the field, typically from the oldest to youngest deposits.

3 FACIES

3.1 Deformed Sand Facies

3.1.1 Description:

Deformed massive sand occurs at the base of section VS-4, which is the lower of the two sections measured in the northeasternmost area of the gravel pit. This deformation occurs as flame structures and ball and pillow sand load structures in very fine sand (Figure 9) in a bed 0.7 m thick. The lower contact of this bed is below the base of the section; therefore, it is unknown how far this deformation extends. No other sedimentary structures are noted in this facies. This deformed sand facies is overlain by a discontinuous, red clay layer that sinks into the underlying deformed sand. These deformation features (Figure 10) cannot be traced laterally to the south or west.

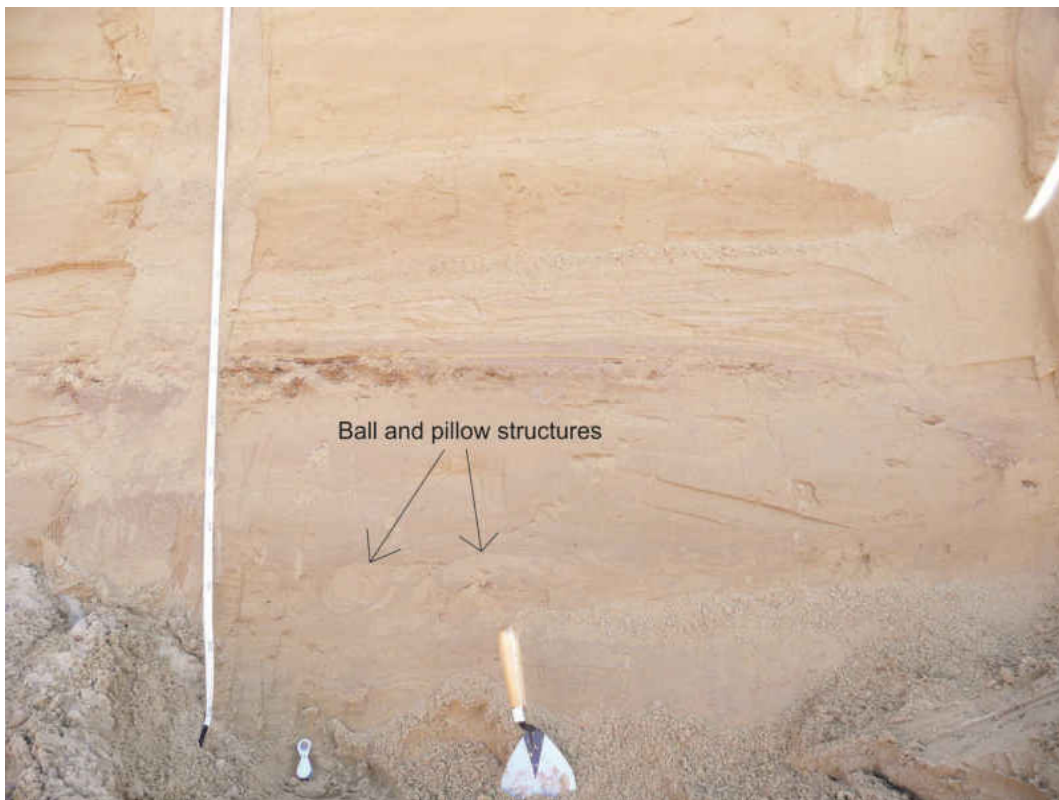


Figure 9. (A) Photograph of deformed sand in section VS-4. Hand lens for scale; (B) Previous photograph with deformation structures highlighted.



Figure 10. Photograph of deformed sand.

3.1.2 Interpretation:

Flame and load structures form when dense sediment is deposited on a water-saturated substrate of lower density. This density inversion results in failure of the substrate and allows the upward escape of water and low-density sediment, while the higher density deposits form bulbous load structures as they sink into the underlying material (Reineck and Singh, 1980). Such features form under conditions of high sedimentation rates in areas where the sediment is shocked either by seismic activity or an overlying current (Reineck and Singh, 1980).

Flame structures are dewatering structures, and occur when denser, wet sediment is loaded onto less dense underlying sediment. The increased weight encourages fluid escape upwards towards the surface (Reineck and Singh, 1980). Sedimentation at this time would likely have occurred as a flow containing a very high sediment concentration known as a hyperconcentrated flow (see also 3.5 Deformed Facies).

3.2 Symmetrical-Rippled Facies

3.2.1 Description:

Symmetrical ripples occur in sections VS-1, VS-2, and VS-3, in the southernmost sections of the pit, and they also occur as single to thin horizons within the lower portion of sections on the north side of the pit. They occur in very fine to medium sand, in beds 10 cm to 1.7 m thick, often alternating with climbing symmetrical (Figure 11) and asymmetrical ripples (Figures 11, 12, 13). Many of the asymmetrical ripples display rounded crests (Figure 14). These climbing ripples display a low to high angle of climb. In some cases, symmetrical ripples are overlain by silt to very fine sand drapes, with the exception of the uppermost symmetrical ripples occurring in sections VS-1 and VS-2, where no drapes occur. Contacts in this facies are gradational to sharp. No erosional contacts are noted in this facies, although a scour surface occurs in section VS-1 (Figure 15), the easternmost section. Red clay clasts occur below the scour surface in VS-1, and throughout VS-3, the westernmost section (Figure 16). No limestones, outsized clasts, or deformational structures were noted in this facies. Paleocurrent orientations taken from the climbing asymmetrical ripples vary between 215.0° and 270.0° (Appendix A).

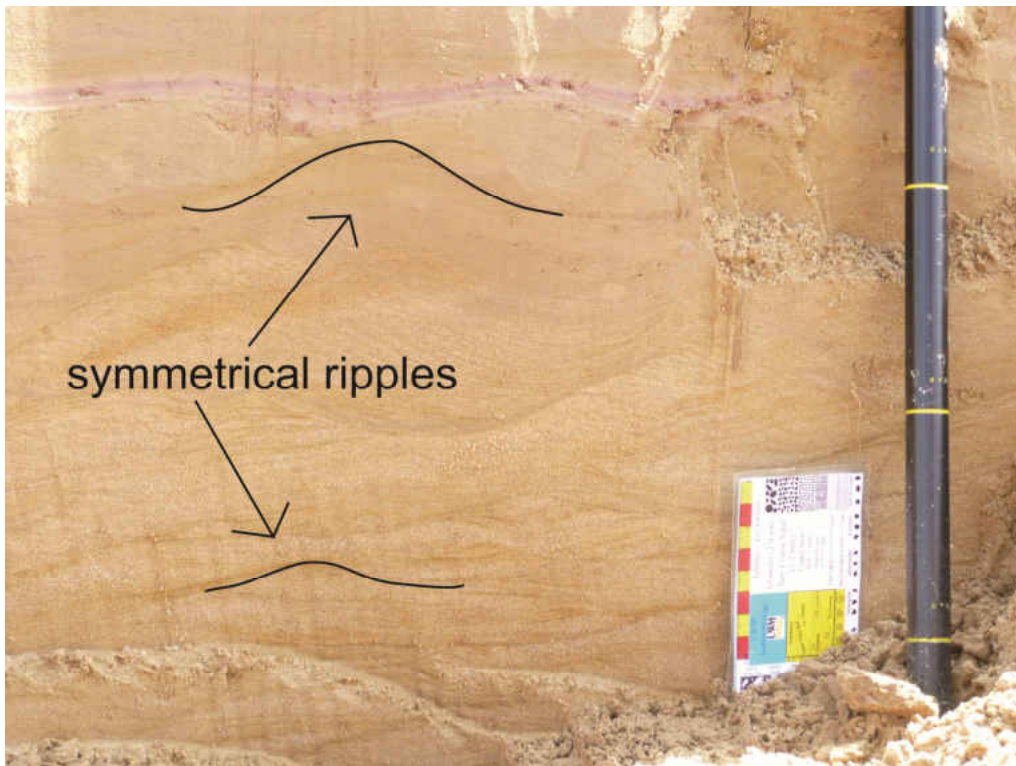


Figure 11. (A) Photograph of climbing symmetrical ripples occurring beneath red clay layer in section VS-1. Yellow horizontal markings in Jacob's staff are 0.1 m apart; (B) Previous photograph with symmetrical ripples highlighted.



Figure 12. Photograph of symmetrical ripples overlain by cross-bedded sand in section VS-2. Field notebook (7.5 cm in length) for scale.



Figure 13. Photograph of alternating symmetrical and climbing ripples in section VS-3. Pen for scale.

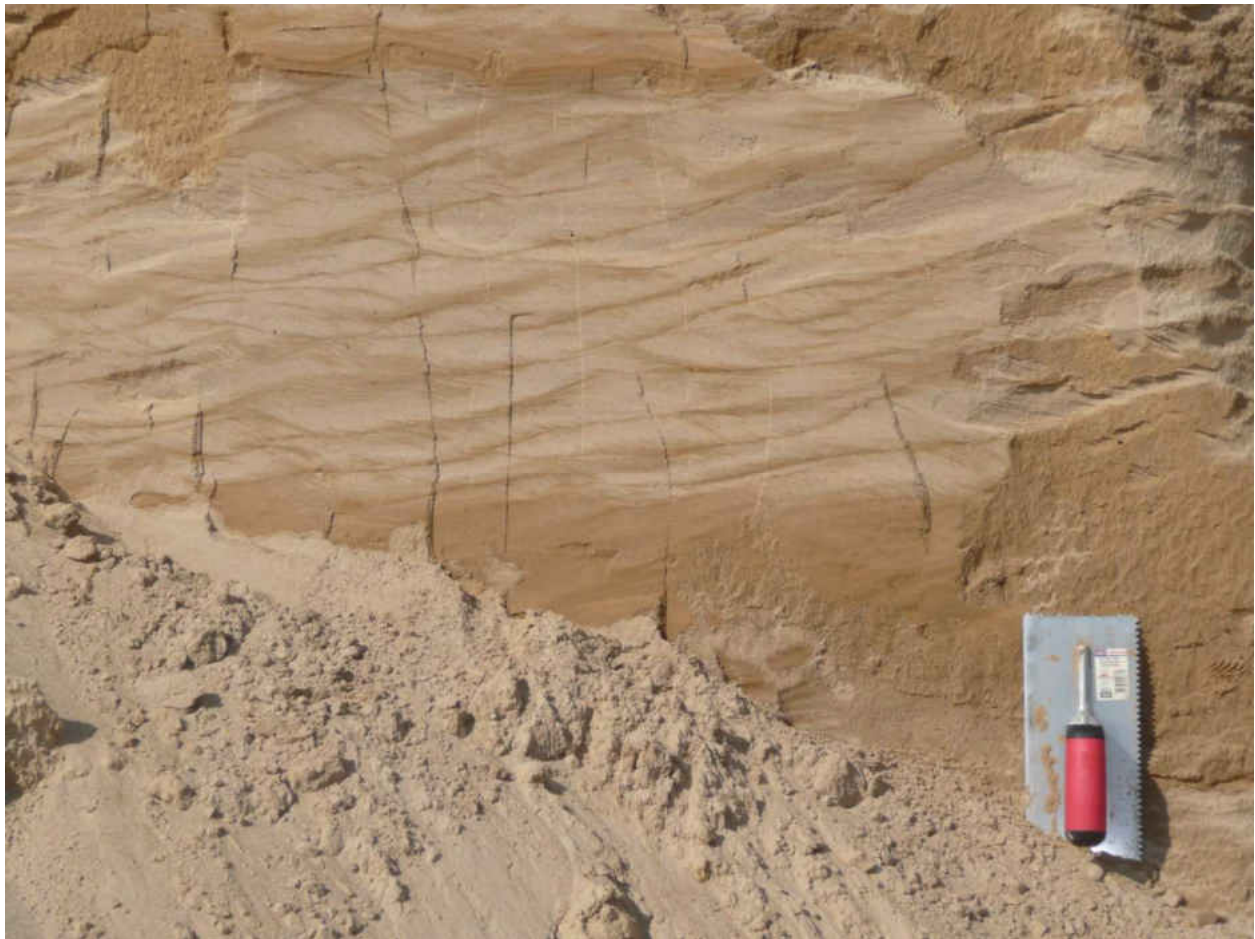


Figure 14. Photograph of alternating symmetrical and climbing ripples in section VS-3. Note rounded ripple crests. Trowel for scale.



Figure 15. Photograph of symmetrical-rippled sand in section VS-1.



Figure 16. Photograph of red clay clasts occurring with Symmetrical-Rippled Facies deposits in section VS-1. Numbers on ruler are 1 cm apart; entire ruler is 30 cm in length.

3.2.2 Interpretation:

These interbedded symmetrical and asymmetrical ripples are interpreted to be wave to combined flow ripples contained within a shallow, standing body of water. Symmetrical ripples form when wind activity produces oscillatory wave activity in shallow-water bodies (Reineck and Singh, 1980). Asymmetrical ripples form from either unidirectional current activity or due to wave activity where there is a net migration direction (Reineck and Singh, 1980). The interbedded nature of the symmetrical ripples with asymmetrical ripples suggests the occurrence of both wave and current activity, and the rounded crest of the asymmetrical ripples suggests that combined flow conditions of both wave and current activity were

occurring simultaneously (Reineck and Singh, 1980; Dumas et al., 2005). Climbing ripples occur under conditions of high sedimentation rates where ripple migration rates are decreasing in a downflow direction. This allows ripples to overtake and climb up the back of the ripple directly in front of them. Commonly, this occurs where flow velocity decreases in a downflow direction, which is typical of areas where confined flow is transitioning into unconfined flow, such as where water enters a standing body of water (Reineck and Singh, 1980). Reactivation surfaces occur in sections VS-1 to VS-2, where symmetrical ripples are overlain by finer-grained drapes, a scour surface, and/or higher energy bedforms (i.e., dunes or climbing ripples). This suggests low energy intervals within the standing body of water where clay settled from suspension followed by either current, wave, or combined flow activity. The absence of dessication cracks within these drapes suggests that the clay was not exposed to the atmosphere, which is consistent with the interpretation of deposition of this facies within a lacustrine setting. Paleocurrent measurements for the asymmetrical ripples indicate water flow direction was from the northeast towards the southwest.

3.3 Unidirectional Bedform Facies Assemblages

3.3.1 Description:

Cross-laminations and/or asymmetrical ripple cross-laminations/marks occur in very fine to medium-grained sand in sections VS-1, VS-2, VS-3, VS-4, VS-5, and VS-6, in beds 0.2 to 2.6 m thick. These cross-laminations sometimes occur as climbing ripples and exhibit a low to high angle of climb. Both climbing ripples and non-climbing ripples occasionally are overlain by mud drapes. No desiccation cracks are noted within these drapes. Grain sizes fluctuate between

beds; however, beds appear to frequently coarsen upwards, both within a bed and between individual beds.

Cross-beds occur in fine to coarse-grained sand in sections VS-2, VS-4, VS-5, VS-7, VS-8, and VS-9 (Figure 17). Both planar and trough cross-beds occur, but never together within the same section. The grain sizes of these cross-beds do not appear to vary within any given section, with the exception of the occurrence of gravel within the middle portion of cross-beds of section VS-5. Overtuned cross-beds occur in medium sand at the top of section VS-8 (Figure 18).

Horizontally-laminated sand occurs in fine sand near the top of section VS-6, overlying climbing ripples in fine sand and underlying asymmetrical ripples in very fine sand.

For all Unidirectional Bedform Facies Assemblages structures, some structures display climbing ripples and climbing dune-like forms. These climbing cross-stratifications occur at both low to high angles of climb. They also occur in macroforms as downclimbing structures, or downstream accretion, approximately 0.5 m high and 4 m long (Figure 19). Such macroforms may also display an angle of climb as they were observed to climb up the back of other macroforms (Figure 20).



Figure 17. Photograph of cross-bedding in sand in section VS-2. Flow direction was from left to right. Brunton compass for scale. Note slight angle of climb and downclimbing or downstream accretion to the right of the staff.

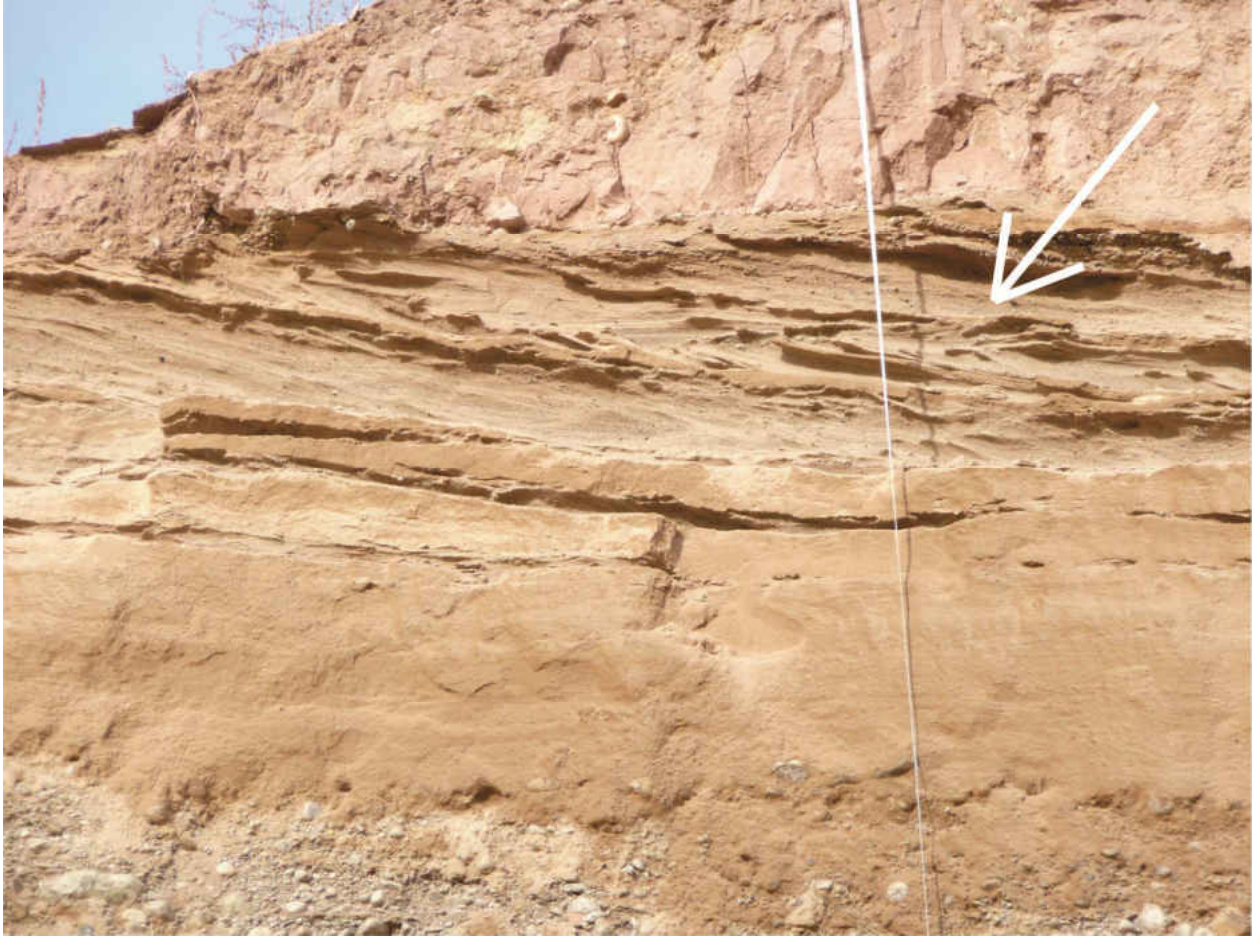


Figure 18. Photograph of overturned cross-beds (white arrow) at the top of section VS-8. Thickness of bed is approximately 1 m. Flow direction at the time of overturning was from left to right.



Figure 19. Photograph of a macroform (bar) made of downclimbing ripples.



Figure 20. Photograph of downstream-accreting macroforms with a low angle of climb to the left (west).

3.3.1a Cross-bedded Sand with Faulting Description:

Both normal (Figure 21, 22) and reverse (Figure 21, 23) faulting occur in cross-bedded sand in an area between sections VS-9 and VS-10. Approximately 16 normal faults were identified but only two reverse faults were located. These faults occur in close proximity to each other, with normal faults dipping at a similar angle, approximately 30°. The reverse faults dip at an angle of approximately 50°.



Figure 21. (A) (left) Photograph of normal and reverse faults in cross-bedded sand. Jacob's staff for scale; (B) (right) Previous photograph with normal faults (green) and reverse faults (red) highlighted.



Figure 22. Photograph of faulting in sand in an area between sections VS-9 and VS-10.



Figure 23. Photograph of reverse faulting in sand between sections VS-9 and VS-10. Trowel for scale.

3.3.2 Interpretation:

These bedforms are interpreted to be from unidirectional flow in an overall increasing energy environment. As flow velocity increases, bedforms transition from cross-laminated ripples to cross-bedded dunes to a horizontal plane bed in some sections (Reineck and Singh, 1980). The increase in grain size corresponds to an increase in flow velocity and is a common occurrence in progradational system. Climbing ripples indicate increased sedimentation rates when bedforms don't have time to migrate before additional bedforms climb up the back of and overtake existing ones (Reineck and Singh, 1980). Such features occur where there is a decrease in flow velocity and/or a decrease in the rate of migration in a downflow direction, often when flow transitions from confined to unconfined. Flow velocity must have been

fluctuating for transitions between bedforms and grain sizes to occur. The occurrence of mud drapes indicates lower energy intervals where finer-grained sediment had time to settle from suspension. The absence of desiccation cracks within drapes suggests mud-draped ripples were never subaerially exposed, which is consistent with the interpretation of subaqueous deposition within a standing body of water (i.e., within a lacustrine setting). The occurrence of ripples above these mud-draped bedforms indicates flow reactivation. The occurrence of gravel within cross-bedded sand near the top of section VS-5, along with overturned cross-beds at the top of section VS-8, also suggest energy was increasing, or that flow was coming from a different point source out of the glacier. Overall, this environment was transitioning from a lower energy environment to a higher one, with paleocurrent measurements indicating water flow direction was towards the west to southwest. The paleocurrents measured in section VS-6 suggest flow was towards the south to southeast.

3.3.2a Cross-bedded Sand with Faulting Interpretation:

Normal faulting is indicative of an extensional environment, whereas reverse faulting is indicative of a contractual one. The occurrence of both normal and reverse faulting within close proximity to each other makes interpretation of this area particularly challenging. However, the dominance of normal faulting suggests an environment of extension was the prevailing control in this area. This could have been the result of slumping and the formation of growth faults or collapse due to the melting of ice, possible in the form of permafrost long after this facies was deposited.

3.4 Gravel Facies

3.4.1 Description:

Gravel occurs in sections VS-7, VS-8, and VS-9 (Figure 24) and consists of clast-supported granule, pebble, and less commonly, cobble beds 0.15 to 1.2 m thick or as clasts in pebbly sand units. Rare boulders occur mid-section in VS-8. The Gravel Facies overlies the Unidirectional Bedform Facies Assemblages described in the previous section and is capped by either massive medium-fine sand or diamicton. Gravel is also interbedded with cross-beds of the Unidirectional Bedform Facies Assemblages, and grades laterally into sands within this facies. In section VS-9, gravel represents the top of the section. Grain size varies within gravel beds and between them, with the maximum clast diameter measured between pebble beds ranging between 7 and 30 cm. Trough cross-bedding occurs in gravel in sections VS-7, VS-8, and VS-9, in grain sizes ranging from granules to pebbles. Cross-bedded gravel occurs almost exclusively in section VS-7, the easternmost gravel-containing section, with maximum clast diameter coarsening upwards and a mean paleocurrent orientation measurement of 288°. The gravel in this section is capped by diamicton. Moving towards the northwest, cross-bedded gravel and sand deposits display a low-angle of climb in the downflow direction (Figures 25, 26, 27). This climb continues laterally where cross-bedded gravel transitions into interbedded cross-bedded medium to coarse-grained sand. Paleocurrent orientation measurements in this area transition from 260° to 305° moving upwards in the section. Interbedded sand occurs rarely in section VS-7 and frequently in section VS-9, with VS-9 being the westernmost of the gravel sections. No interbedded sand occurs in section VS-8. Cross-bedding in gravel is notably absent in grain sizes larger than pebbles, and in areas where beds are better-sorted. Overall, the gravel in all of

these sections appears to coarsen upwards, except where it is overlain by sand as along the western side of the exposure.



Figure 24. Photograph of Gravel Facies (containing sections VS-7, VS-8, and VS-9 from right to left). Backpack in lower right corner for scale.



Figure 25. Photograph of gravel dipping upstream. Tape measure placed for measurement of section VS-8. Entire section measures 6.2 m in height. Backpacks for scale.



Figure 26. Photograph of cross-bedded gravel in section VS-8. Entire section measures 6.2 m in height.



Figure 27. Photograph of cross-bedding in gravel in section VS-8. Jacob's staff for scale.

3.4.2 Interpretation:

These gravel beds are interpreted to be from unidirectional flow in an overall increasing energy environment. As is the case in the previous section, as flow velocity increases, grain size increases, transitioning from cross-bedded granules and pebbles to massive cobbles with rare boulders (Reineck and Singh, 1980; Cutler et al., 2002). This increase in grain size does not support the continuation of cross-bedding. Coarser and more abundant bedload allows a steeper frontal profile. Interbedded sand and gravel in the downflow direction suggest flow is changing from confined to unconfined flow or intermittent flow with reactivation and lower energy intervals. Climbing bedforms are also likely climbing macroforms. Flow in this area could

have been transitioning from confined to unconfined or affected by a rise in base level, causing a decrease in velocity in the downflow direction. Paleocurrent orientation measurements suggest flow was towards the west to west-northwest.

3.5 Deformed Facies

3.5.1 Description:

Several types of deformed strata occur in the Tower Hill sand and gravel pit including: flame and load structures (see 3.1 Deformed Sand Facies), soft sediment faulting (see 3.3 Unidirectional Bedform Facies Assemblages), and large-scale folding and faulting that is described here in the Deformed Facies. Large-scale deformation occurs in section VS-10, and in an area between sections VS-9 and VS-10, which contains the majority of deformed deposits. The Deformed Facies is overlain by the Diamict Facies. Deformed strata occur along the northwestern wall of the pit and are associated with two major truncation surfaces (Figure 28). Early photos of the pit walls aid in the identification of these features. The first truncation surface separates undeformed facies of the Unidirectional Bedform Facies Assemblages and Symmetrical-Rippled Facies below from undeformed and partially deformed facies above. This surface defines a trough-shaped depression approximately 10 m deep and greater than 50 m wide (Figure 28).



Figure 28. (A) (top) Photograph of the deformed area in 1997. Photograph provided by Dr. William Mode. Truck for scale; (B) (bottom) Figure 28A with truncation surfaces 1 and 2 annotated.

The surface displays both a relatively smooth, gently-dipping profile and, in places, steep, step-like truncation of the underlying sand (Figure 29).



Figure 29. Photograph of steep steps on truncation surface. Geologist for scale.

Stratified and cross-bedded gravel overlies this surface and drapes the underlying depression. The gravel is composed of pebble and cobble clasts of dolomite with rare dolomite boulders and, in places, angular blocks of stratified sand up to 0.4 m in length (Figures 30, 31).

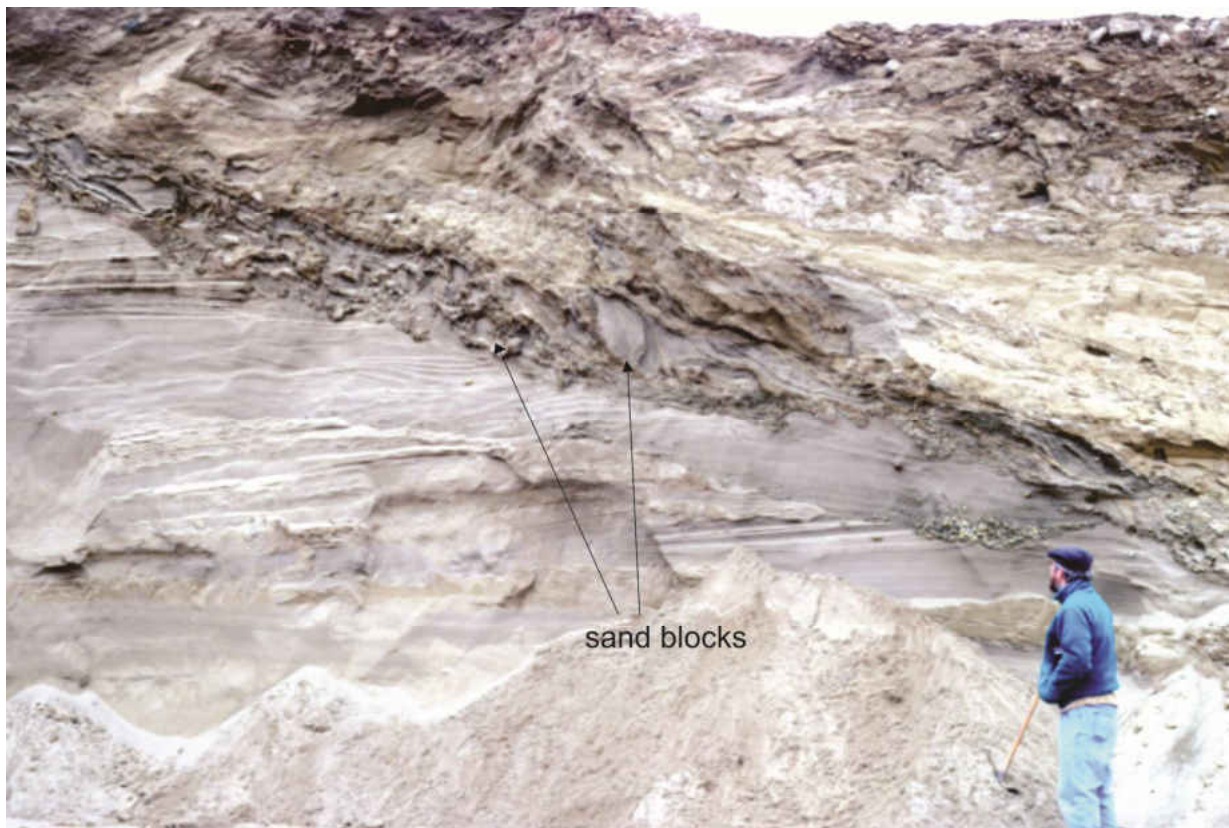


Figure 30. Photograph of sand blocks exposed in 1997. Photograph provided by Dr. William Mode. Geologist for scale.



Figure 31. Photograph of sand blocks in gravel.

Upward, the gravel interfingers with, and is overlain by, sand. The top of this succession is deformed and, in some places, incorporated into the deformation associated with the overlying truncation surface. A second truncation surface occurs above the gravels and in some places may downcut to and merge with the first truncation surface (Figure 28). This second truncation surface is also a trough-shaped depression superimposed upon the first. However, the second truncation surface extends beyond the underlying depression and forms several other depressions along the length of the exposure. In most places in the pit, this surface separates diamict above from undeformed strata below. However, within the area between sections VS-9 and VS-10 (Figure 32), the depression created by the second truncation surface is

filled by deformed admixtures of gravel, sand, silt, clay, and diamict. In places, gravel and sand contained in the depression overlying truncation surface 1 is incorporated into the overlying deformation faces (Figure 28). Deformation occurs as isolated and discontinuous, deformed bodies characterized by deformed rafts of sand and gravel, recumbent folds, sheath-like folds, nappe-like structures, thrust-faulted blocks, and blocks of relatively undeformed strata floating in the sediment admixture (Figures 32, 33). Red clay, displaying fissility, appears to have been sheared into the sequence. The deformed zone is overlain by and interfingers with undeformed matrix-supported, clast-poor red diamict.



Figure 32. Photograph of main area of deformation between sections VS-9 and VS-10. Geologist for scale.



Figure 33. Photograph of area near section VS-10 with an overturned front, sheath-fold, and nappe-like block.



Figure 34. Photograph of folding in sand and gravel between sections VS-9 and VS-10.

3.5.2 Interpretation:

The Deformed Facies was deposited after all other facies with the exception of the Diamict Facies.

Deformed beds cause a challenge to interpretation (Evans et al., 2006) as they cannot simply be correlated straight across exposures, and because they occur in a relatively small area of the pit. Truncation surface 1 is overlain by thick beds of cross-bedded gravel and sand. The occurrence of sand with steep step-like features on the truncation surface along with cross-bedded gravel containing sand blocks suggest this surface truncated frozen sediment. These blocks were likely not carried relatively far as, even frozen, they would not have survived intense water abrasion in a flow capable of transporting gravel. Such features strongly suggest that the sediment underlying truncation surface 1 was subaerially exposed in order for it to become frozen. The truncation of unfrozen sediment would have produced a smoother truncation surface and not have allowed the preservation of temporarily consolidated sand blocks in what would later become unconsolidated sediment.

Truncation surface 1 is an incision surface that was produced by stream flow. This is suggested by the presence of traction features within its fill (e.g., cross-bedded gravel). Such surfaces can be created by either a fall in base level (i.e., a lowering of lake level) (Emery and Myers, 1996; Posamentier and Allen, 1999; Catuneanu, 2006) or an increase in stream power (Blum and Törnqvist, 2000; Gruszka, 2001). Incision into underlying lake deposits of the Symmetrical-Rippled Facies, which appear to have been frozen and subaerially exposed at the time of incision, suggests that a fall in base level is the more likely explanation for production of the truncation surface.

Truncation surface 2 appears to have been produced by deformation: the admixture of gravel, sand, silt, clay, and diamict could be the result of slumping or glaciotectonic deformation. The complexity of these deposits suggests extensive deformation. Slump blocks result from the intact sliding of sediment. Slump features include, but are not limited to: contorted bedding, small-scale faults, rotated and inverted blocks, overturned folds, thrusting (at the downslope or “toe” end), nappe-like features, and curved, concave upward fault planes (Reineck and Singh, 1980). Deformation due to glacial tectonics would have been the more likely cause of features in this facies, as slumping would not produce superimposed styles of different types of folding (Barrett, 1972; Moore et al., 2011), and different orientations of sediment rafts, nappe-like structures, or sheath(-like) folds (Croot, 1988; McCarroll and Rijdsdijk, 2003). The occurrence of thrust sheets in silt, along with the fissility of sheared clay suggest compression caused by ice shove (Benn and Evans, 1998; Henriksen et al., 2001; Isbell, 2010; Moore et al., 2011). Additionally, the Deformed Facies being immediately overlain by the Diamict Facies suggests close proximity of the glacier. Ice shove would have occurred as the ice front overrode this area, deforming much of the underlying sediment. Diamict is most commonly deposited along the ice margin and in a subglacial position, with deposits having a better chance of preservation during periods of ice recession. The immediate subsequent deposition of diamict suggests the ice margin was already nearby, and would be the anticipated vertical transition in the depositional succession.

3.6 Diamict Facies

3.6.1 Description:

The Diamict Facies occurs above the Unidirectional Bedform Facies Assemblages and Deformed Facies (Figure 35) and, in the gravel pit, is not overlain by any other deposits. This unit is 0.5 m to several meters thick and consists of a red, clay-rich, matrix-supported, clast-poor diamict. The clasts consist of dolomite and granite ranging from granule to cobble-sized clasts. Although not observed in place, boulder-sized clasts are also likely due to the occurrence of clasts of that size within the sand and gravel pit. The diamict rises and falls over relief on truncation surface 2 and, in most places, appears to drape underlying deposits except near the depression cut by the truncation surface between sections VS-9 and VS-10. The diamict was largely inaccessible in the sand and gravel pit due to its location being at the top of the pit walls. However, photos of the diamict suggest that, in places, it had a fissile-like appearance.



Figure 35. Photograph of diamict overlying sand and gravel in an area between sections VS-9 and VS-10.

3.6.2 Interpretation:

The diamict that caps the deposits of sand and gravel in the pit is interpreted here to be glaciogenic and deposited during the deposition of the Glenmore glacial phase. The fissility displayed by the clay suggests it was sheared (Bradley and Hanson, 1998). The deformation suggests that glaciotectonics occurred during ice advance, which is common on permafrost (Golledge and Phillips, 2008). This interpretation is in agreement with Mickelson and Mode (2007), who suggested that the red clay of the Chilton Member was sheared into the overlying sand and gravel deposits.

4 ENVIRONMENTAL DISCUSSION

The deposits of the Tower Hill sand and gravel pit were deposited when cold, glacial meltwater entered glacial Lake Oshkosh. Evidence for a standing body of water in this region is

provided by the occurrence of wave-ripple laminations contained throughout the base of the stratigraphic succession found in the gravel pit (see 3.2 Symmetrical-Rippled Facies). Mickelson and Mode (2007) interpreted the sand in the lower portion of the pit to have been deposited by a delta built towards the southwest between ice and the Silurian escarpment. They based their evidence on the occurrence of low-angle, southwestward dipping beds of sand and fine gravel. Such beds were not observed in the pit during this study. Instead, in many places, beds were observed to dip gently upflow towards the northeast; thus, raising the possibility that water entered the lake as part of a grounding-line fan system. In a deltaic system, the ice front would have been separated from the lake by a braided outwash plain, whereas, in a grounding-line fan system, the ice would have been in direct contact with lake waters. Regardless, evidence of meltwater entering the lake from the northeast is provided by southwestward-directed paleocurrents and the occurrence of trough cross-laminations, climbing asymmetrical ripples, and cross-bedded sands and gravels of the Unidirectional Bedform Facies Assemblages and Gravel Facies. This flow likely would have been either hyperpycnal or homopycnal upon entering the lake, as both the incoming glacial meltwater and glacial Lake Oshkosh would have been characterized by similar temperatures and salinities. The sediment load carried by the incoming glacial meltwater could have made this flow slightly more dense (Bell et al., 1999; Miall, 1976). Therefore, the initial assumption of a hyperpycnal underflow is not unreasonable. Ground penetrating radar (GPR) data display a slope that is consistent with those measured in the field by other means (e.g., photographs and stratigraphic sections) (Figures 36, 37).



Figure 36. Photographs and associated ground penetrating radar (GPR) data of the Tower Hill sand and gravel pit collected by Dr. William Kean in 2010. View is towards the north-northeast. Geologists for scale. See Appendix E for additional metadata.

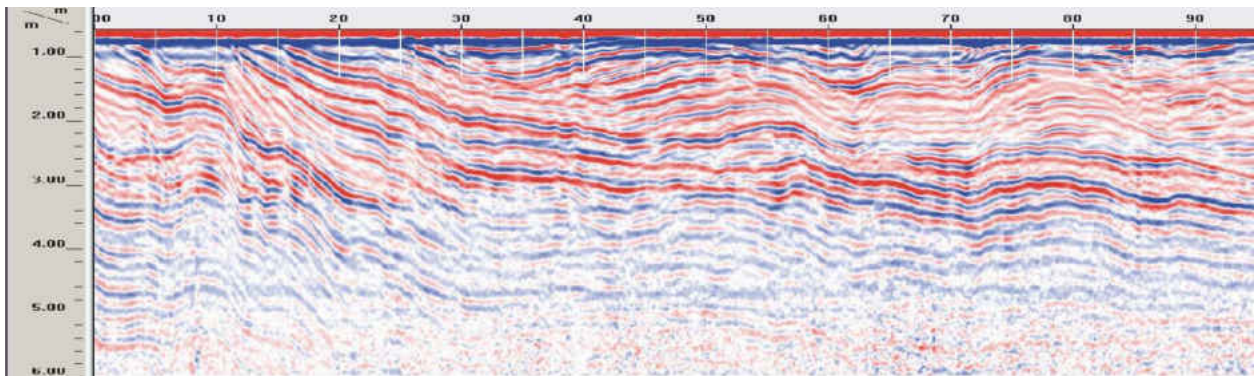


Figure 37. GPR profile on upper terrace of the Tower Hill sand and gravel pit to 6 m depth collected by Dr. William Kean in 2010. See Appendix E for additional metadata.

Deltas are depositional features with subaerial components: distributary channels, levees, emergent crevasse splays, and delta plains/braid plains (Snedden, 2006). Deltas also have subaqueous portions, which contain a delta mouth bar, delta front, and prodelta environments (Scruton, 1960; Snedden, 2006). Deltas form when confined stream flow enters a standing body of water (McPherson et al., 1987; Galloway, 2006). As the incoming water transitions from confined to unconfined conditions, velocity drops and deposition of the

coarsest-grained sediment of the transported load occurs. The resulting characteristics of a delta depend on the density contrasts between the two bodies of water, the bathymetry between the distributary channel and lake bottom, and their energy dynamics (wave, fluvial, or mixed-influence) (Galloway, 1975; Miall, 1976). Nonmarine deltas typically form “Gilbert-type” deltas consisting of bottomset, steeply-dipping foreset, and topset beds (Lønne, 1995; Kostic et al., 2005; Winsemann et al., 2007). Climbing ripple marks are common on dipping foreset and bottomset beds, where stream discharge changes from confined to unconfined. The dipping foreset beds are the river mouth bar; the topset beds are composed of fluvial and delta plain deposits. Where preserved, the vertical distance between the bottomset and topset beds provides reliable measurements of water depth (Bhattacharya, 2006).

Deltaic systems in glacial settings are often accompanied by braided outwash plains that connect a terrestrial (i.e., not ending in a standing body of water) ice front with a Gilbert-type delta (McPherson et al., 1987). Such deposits are typically composed of gravel and coarse sand with the orientation of the beds being horizontal. Upstream-dipping beds could be produced if base level (i.e., lake level) was rising; however, in such cases, flooding across the low relief plain would be expected (Catuneanu, 2006).

Grounding-line fans are subaqueous, depositional features that form from subglacial meltwater discharge along a glacial ice front that ends within a standing body of water. These typically form as crescent to lobate-shaped fan-like bodies that grow upward and outward as deposition continues (Powell, 1990). The transition from confined to unconfined flow results in decreasing flow velocities outward away from the mouth of a subglacial conduit, which in turn results in climbing bedforms and macroforms as both small-scale and large-scale flow features

migrate up the back of the proximal growing fan surface. In the field, stratification dips in the “upstream” direction. On the “downstream” side of the fan, beds may dip in a “downstream” direction as the fan progrades away from the ice front. Grounding-line fans may transition into deltas if the fan surface eventually builds upward far enough to take on a subaerial component (Powell, 1990).

In the Tower Hill sand and gravel pit, the occurrence of the interfingering Symmetrical-Rippled Facies, and cross-stratified dunes and ripples (including climbing ripples) indicates the juxtaposition of lake and current-dominated inflow systems. The coarsening upward succession of sand into these facies transitioning into gravel deposited by unidirectional flow indicates progradation of a coarse-grained dispersal system. However, the absence of steeply-dipping foreset beds in this study is not consistent with the interpretation of these strata having been deposited in a deltaic system. Instead, the sand in the lower portion of the pit (see 3.3 Unidirectional Bedform Facies Assemblages) and the gravel in the upper portion of the pit (see 3.4 Gravel Facies) display beds that dip in the “upstream” direction, suggesting that these beds were deposited in either a grounding-line fan system that coarsened upward as progradation and up-building proceeded, and/or on a late-stage braid plain where base level was rising, resulting in aggradation of the sediment system (Figure 38A).

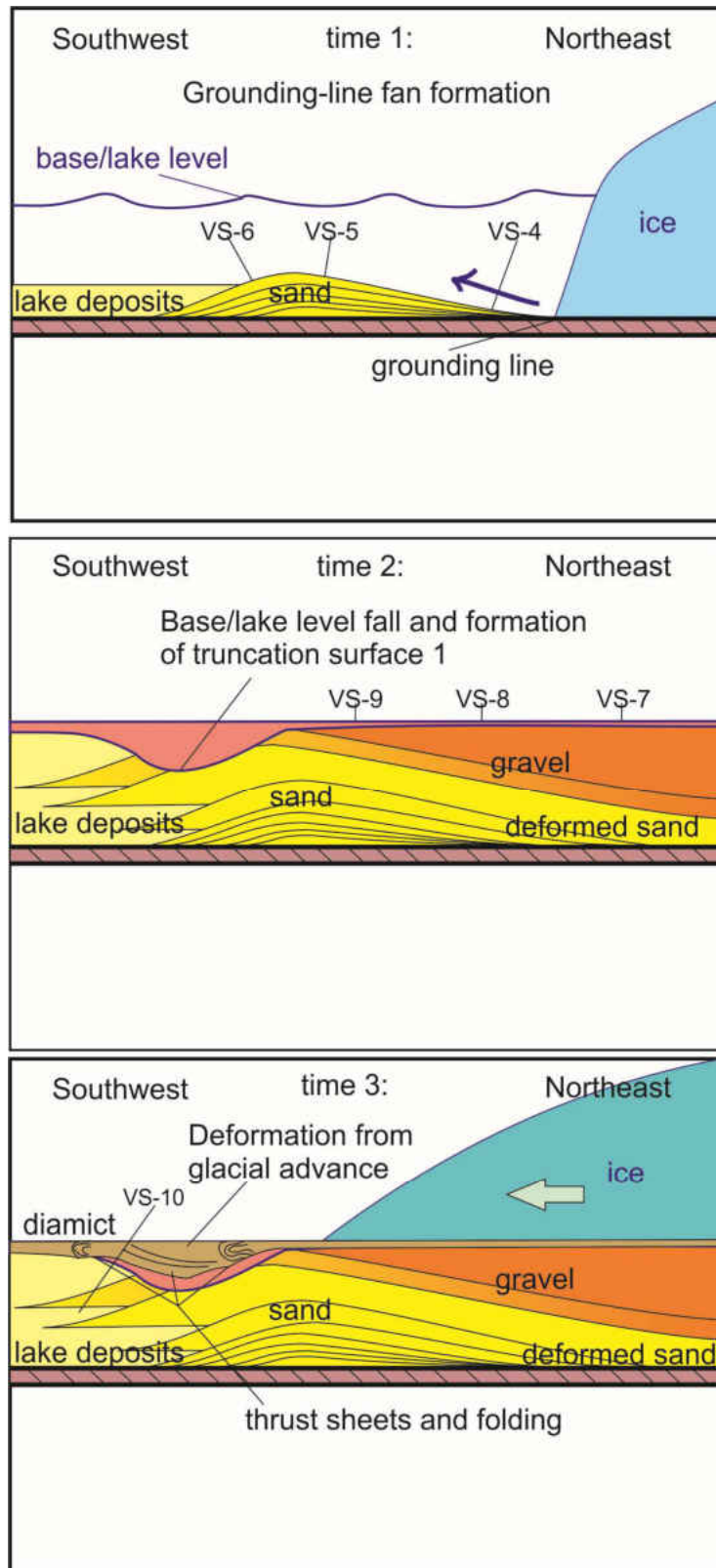


Figure 38. Schematic cross sections of interpretation of deposition and lake/glacial dynamics occurring over time: (A) (top) Initial grounding-line fan-building phase; (B) (middle) base level fall and formation of truncation surface 1; and (C) (bottom) ice shove.

In the first scenario, a grounding-line fan system, the standing body of water would have been in direct contact with the lake. If this occurred, icebergs should have calved off of the ice front, with the formation of keel marks due to iceberg grounding on the shallow bottom, and ice-rafted debris melted out of and dumped off of the iceberg should have been an important component in a shallow lake with the substrate located above wave base. In the second scenario, a braid plain would have ended in a delta, and rising base level should have resulted in flooding of lake deposits on top of the gravels. Because ice was likely receding, it is probable that lake levels may have been slowly rising throughout deposition of the deposits and that perhaps both of the above scenarios may have occurred, which could explain observations in the sand and gravel pit. Therefore, both interpretations may have merit. In either case, it is not possible to accurately determine water depth, as it likely varied during the duration of sedimentation of the lower succession.

The first truncation surface, with its incision into underlying lake deposits, indicates a fall in base/lake level or an increase in stream power. Either process can result in incision (Blum and Törnqvist, 2000). The occurrence of sand blocks in gravel and steep step-like features along this truncation surface provides supporting evidence that the underlying sediment was frozen at the time the first truncation surface formed. The occurrence of both of these features suggests that the underlying “lake” deposits were subaerially exposed, which supports the hypothesis that lake levels were falling (Figure 38B). Northward recession of the ice front may have resulted in the activation of a nearby drainage outlet, allowing the partial draining of glacial Lake Oshkosh, and incision of stream flow to occur as lake levels fell (Brookfield and Martini, 1999; Hooyer, 2007).

The second truncation surface appears to have been produced by extensive deformation as the result of glacial tectonics. The combination of thrust sheets in silt, superimposed styles of different types of folding, and different orientations of sediment rafts, nappe-like structures, and/or sheath(-like) folds is consistent with deformation as ice shove along an ice front that overrode this site. The Diamict Facies immediately overlying the Deformed Facies further suggests that the glacier was in close proximity and overrode the location of the Tower Hill pit, as glaciogenic diamict tends to be deposited along ice margins and in subglacial positions (Benn and Evans, 1998).

The reexamination of deposits preserved in the Tower Hill sand and gravel pit are interpreted here to be those of a grounding-line fan deposited subaqueously, which differs from the interpretation of a prograding delta by Mickelson and Mode (2007). Reinterpretation suggests that a grounding-line fan occurred in the eastern portion of the original pit, with the lake being southwest of the grounding-line, and that glacial Lake Oshkosh during the time of the Glenmore glacial phase was an ice-contact lake. Due to the absence of Gilbert-type deltaic deposits, actual water depth of former glacial Lake Oshkosh in the area of the Tower Hill sand and gravel pit at that time could not be determined. However, the occurrence of wave ripples throughout the basal deposits of the pit suggests water depth was relatively shallow. Additionally, the production of truncation surface one suggests lake level fell significantly at least once, due to activation of a drainage outlet. The deformation that occurs towards the northwest corner of the gravel pit is interpreted here to be from ice shove (Figure 38C).

5 CONCLUSIONS

Reexamination of the deposits of the Kewaunee Formation in the Tower Hill sand and gravel pit near De Pere, Wisconsin suggests these deposits were those of a grounding-line fan with its deposits building towards the southwest. The ice was dynamic at this time as evidenced by the occurrence of a relatively large truncation surface, interpreted to have been from a fall in base/lake level, suggesting the opening of a previously blocked drainage outlet elsewhere in the basin due to recession of the ice front to the north-northeast. The occurrence of wave ripples found as basal deposits in most sections suggests that water depth, although not measurable, was relatively shallow. The occurrence of the aforementioned truncation surface also suggests that water depth was not fixed, but changing over time. Deformation in the northwest corner of the pit occurred by glaciotectonics, specifically ice shove, as evidenced by thrust sheets in silt, superimposed styles of different types of folding, and different orientations of sediment rafts, nappe-like structures, and/or sheath(-like) folds. The ice margin would have been nearby to have deformed these deposits by ice shove and subsequent deposition of the Diamict Facies indicates that the area was overridden by ice during a readvance of the ice front relatively soon after.

The previous interpretation of these deposits as those of a Gilbert-type delta (Mickelson and Mode, 2007) could not be substantiated at the time of this study due to the absence of steeply-dipping foreset beds.

This site contains a record of ice-lake interactions during deposition of the Chilton Member, and thus, helps resolve the ice readvance and recession history of the Green Bay Lobe during deposition of the Kewaunee Formation.

6 REFERENCES

- Allmendinger, R.W., 2016. Stereonet 9, version 9.6.2. Retrieved from: www.geo.cornell.edu/geology/faculty/RWA/programs/stereonet.html. Date Accessed: 07/09/2016.
- Attig, J.W., Hanson, P.R., Rawling III, J.E., Young, A.R., Cason, E.C., 2011. Optical ages indicate the southwestern margin of the Green Bay Lobe in Wisconsin USA, was at its maximum extent until about 18,500 years ago. *Geomorphology* 130, 384-390.
- Barrett, P.J., 1972. Late Paleozoic glacial valley at Alligator Peak, southern Victoria Land, Antarctica. *New Zealand Journal of Geology and Geophysics* 15.2: 262-268.
- Bell, T., Sheppard, K., Liverman, D.G.E., 1999. Stratigraphy and age of Quaternary sediments exposed along the coast of southern St. George's Bay. Newfoundland Department of Mines and Energy Geological Survey 99, 125-137.
- Benn, D.I., Evans, D.J.A., 1998. *Glaciers & Glaciation*; Oxford University Press Inc., New York, NY, 734 p.
- Bhattacharya, J.P., 2006. Deltas. *SEPM (Society for Sedimentary Geology)* 84, 237-292.
- Black, R.F., 1970. Glacial geology of Two Creeks forest bed, Valderan type locality, and northern Kettle Moraine State Forest. Wisconsin Geological and Natural History Survey Information Circular 13, 40 p.
- Black, R.F., 1980. Valdres—Two Creeks, Wisconsin, revisited: The Valdres Till is most likely post-Twocreekan. *Geological Society of America Bulletin* 91, 713-723.
- Blum, M.D., Törnqvist, T.E., 2000. Fluvial responses to climate and sea-level change: a review and look forward. *Sedimentology* 47, 2-48.
- Bradley, D., Hanson, L., 1998. Paleoslope Analysis of Slump Folds in the Devonian Flysch of Maine. *Journal of Geology* 106, 305-318.
- Brookfield, M.E., Martini, I.P., 1999. Facies architecture and sequence stratigraphy in glacially influenced basins: basic problems and water-level/glacier input-point controls (with an example from the Quaternary of Ontario, Canada). *Sedimentary Geology* 123, 183-197.
- Catuneanu, O., 2006. *Principles of Sequence Stratigraphy*. Amsterdam, Elsevier Science, 375 p.
- Clark, J.A., Befus, K.M., Hooyer, T.S., Stewart, P.W., Shipman, T.D., Gregory, C.T., Zylstra, D.J., 2008. Numerical simulation of the paleohydrology of glacial Lake Oshkosh, eastern Wisconsin, USA. *Quaternary Research* 69, 117-129.

- Clark, P.U., 1992. Surface form of the southern Laurentide Ice Sheet and its implications to ice-sheet dynamics. *Geological Society of America Bulletin* 104, 595-605.
- Colgan, P.M., Mickelson, D.M., 1997. Genesis of streamlined landforms and flow history of the Green Bay Lobe, Wisconsin, USA. *Sedimentary Geology* 111, 7-25.
- Croot, D.G., 1988. Morphological, structural and mechanical analysis of neoglacial ice-pushed ridges in Iceland. *Glaciotectonics: Forms and Processes*, 33-47.
- Cutler, P.M., Colgan, P.M., Mickelson, D.M., 2002. Sedimentologic evidence for outburst floods from the Laurentide Ice Sheet margin in Wisconsin, USA: implications for tunnel-channel formation. *Quaternary International* 90, 23-40.
- Dumas, S., Arnott, R.W.C., Southard, J.B., 2005. Experiments on oscillatory-flow and combined-flow bed forms: implications for interpreting parts of the shallow-marine sedimentary record. *Journal of Sedimentary Research* 75, 501-513.
- Emery, D., Myers, K.J., 1996. *Sequence Stratigraphy*. Blackwell Science Ltd., Oxford, 297 p.
- Evans, D.J.A., Phillips, E.R., Hiemstra, J.F., Auton, C.A., 2006. Subglacial till: Formation, sedimentary characteristics and classification. *Earth-Science Reviews* 78, 115-176.
- Galloway, W.E., 1975. *Process Framework for Describing the Morphologic and Stratigraphic Evolution of Deltaic Depositional Systems*. Houston Geological Survey, 87-98.
- Golledge, N.R., Phillips, E., 2008. Sedimentology and architecture of De Geer moraines in the western Scottish Highlands, and implications for grounding-line glacier dynamics. *Sedimentary Geology* 208, 1-14.
- Gruszka, B., 2001. Climatic versus tectonic factors in the formation of the glaciolacustrine succession (Bełchatów outcrop, central Poland). *Global and Planetary Change* 28, 53-71.
- Henriksen, M., Mangerud, J., Maslenikova, O., Matiouchkov, A., Tveranger, J., 2001. Weichselian stratigraphy and glaciotectonic deformation along the lower Pechora River, Arctic Russia. *Global and Planetary Change* 31, 297-319.
- Hooyer, T.S., 2007. Late Glacial History of East-Central Wisconsin. Guide Book for the 53rd Midwest Friends of the Pleistocene Field Conference, May 18-20, 2007, Oshkosh, Wisconsin. Wisconsin Geological and Natural History Survey Open-File Report 2007-01.
- Hooyer, T.S., Mode, W.N., Mickelson, D.M., Attig, J.W., Forman, S.L., 2009. The deglacial chronology of the Green Bay Lobe, Wisconsin. *Abstracts with Programs – Geological Society of America* 41.4: 22.

- Isbell, J.L., 2010. Environmental and paleogeographic implications of glaciotectonic deformation of glaciomarine deposits within Permian strata of the Metschel Tillite, southern Victoria Land, Antarctica. *Geological Society of America Special Paper* 468, 81-100.
- Kaiser, K.F., 1994. Two Creeks Interstade Dated through Dendrochronology and AMS. *Quaternary Research* 42, 288-298.
- Kostic, B., Becht, A., Aigner, T., 2005. 3-D sedimentary architecture of a Quaternary gravel delta (SW-Germany): Implications for hydrostratigraphy. *Sedimentary Geology* 181, 143-171.
- Lønne, I., 1995. Sedimentary facies and depositional architecture of ice-contact glaciomarine systems. *Sedimentary Geology* 98, 13-43.
- Maher, L.J.Jr., Mickelson, D.M., 1996. Palynological and Radiocarbon Evidence for Deglaciation Events in the Green Bay Lobe, Wisconsin. *Quaternary Research* 46, 251-259.
- McCarroll, D., Rijdsdijk, K.F., 2003. Deformation styles as a key for interpreting glacial depositional environments. *Journal of Quaternary Science* 18, 473-489.
- McCartney, M.C., Mickelson, D.M., 1982. Late Woodfordian and Greatlakean history of the Green Bay Lobe, Wisconsin. *Geological Society of America Bulletin* 93, 297-302.
- McPherson, J.G., Shanmugam, G., Moiola, R.J., 1987. Fan-deltas and braid deltas: Varieties of coarse-grained deltas. *Geological Society of America Bulletin* 99, 331-340.
- Miall, A.D., 1976. Facies Models 4, Deltas. *Geoscience Canada* 3, 215-227.
- Mickelson, D.M., Mode, W.N., 2007. Prograding delta along the eastern edge of glacial Lake Oshkosh, Tower Hill gravel pit, Brown County. In: *Guide Book for the 53rd Midwest Friends of the Pleistocene Field Conference, May 18-20, 2007, Oshkosh, Wisconsin, 2007-01, Open-file report, 41-43.*
- Mills, H.C., Wells, P.D., 1974. Ice-Shove Deformation and Glacial Stratigraphy of Port Washington, Long Island, New York. *Geological Society of America Bulletin* 85, 357-364.
- Mode, W.N., 1989. Glacial Geology of East-Central Wisconsin, in Palmquist, J.C., ed., *Wisconsin's Door Peninsula: Perin Press, Appleton, 66-81.*
- Moore, P.L., Iverson, N.R., Brugger, K.A., Cohen, D., Hooyer, T.S., Jansson, P., 2011. Effect of a cold margin on ice flow at the terminus of Storglaciären, Sweden: implications for sediment transport. *Journal of Glaciology* 57, 35 p.
- Need, E.A., 1983. Pleistocene Geology of Brown County, Wisconsin, map 83-1. University of Wisconsin-Extension Geological and Natural History Survey.

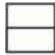

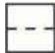

























- Peterson, W.L., 1986. Late Wisconsinan Glacial History of Northeastern Wisconsin and Western Upper Michigan. U.S. Geological Survey Bulletin 1652.
- Posamentier, H.W., Allen, G.P., 1999. Siliciclastic sequence stratigraphy – concepts and applications. *SEPM Concepts in Sedimentology and Paleobiology*, 210 p.
- Powell, R.D., 1990. Glacimarine processes at grounding-line fans and their growth to ice-contact deltas. *Geological Society Special Publications* 53, 53-73.
- Reineck, H.E., Singh, I.B., 1980. *Depositional Sedimentary Environments*, Second, Revised and Updated Edition. Springer-Verlag, New York, 551 p.
- Scruton, P.C., 1960. Delta Building and the Deltaic Sequence. *American Association of Petroleum Geologists*, 82-102.
- Snedden, J.W., 2006. Getting Started in Deltas: A Compendium of Influential Papers. *American Association of Petroleum Geologists*, 1-16.
- Socha, B.J., Colgan, P.M., Mickelson, D.M., 1999. Ice-surface profiles and bed conditions of the Green Bay Lobe from 13,000 to 11,000 ¹⁴C-years B.P., in Mickelson, D.M., and Attig, J.W., eds., *Glacial processes, past and present*, Geological Society of America Special Paper 337, 151-158.
- Syverson, K.M., Clayton, L., Attig, J.W., Mickelson, D.M., 2011. *Lexicon of Pleistocene Stratigraphic Units of Wisconsin*. Wisconsin Geological and Natural History Survey Technical Report 1.
- Thwaites, F.T., Bertrand, K., 1957. Pleistocene geology of the Door Peninsula, Wisconsin. *Geological Society of America Bulletin* 68, 831-880.
- Winguth, C., Mickelson, D.M., Colgan, P.M., Laabs, B.J.C., 2004. Modeling the deglaciation of the Green Bay Lobe of the southern Laurentide Ice Sheet. *Boreas* 33, 34-47.
- Winsemann, J., Asprion, U., Meyer, T., Schramm, C., 2007. Facies characteristics of Middle Pleistocene (Saalian) ice-margin subaqueous fan and delta deposits, glacial Lake Leine, NW Germany. *Sedimentary Geology* 193, 105-129.

APPENDICES

Appendix A: Paleocurrent Measurements

SECTION	ELEVATION ABOVE SECTION BASE (m)	MEASUREMENTS (°)	N	VECTOR MEAN (trend)	VECTOR LENGTH (mean length all)
VS-1	2.0	220, 190, 245, 235, 220, 220, 245, 190, 198	9	218	0.9380
VS-2	2.2-2.5	240, 240	2	240	1.0000
VS-3	0.85	275, 265	2	270	0.9962
VS-3	0.95	190, 240	2	216	0.9063
VS-3	1.0-1.5	225, 235, 240, 240, 225, 230	6	233	0.9940
VS-3	1.7	255, 280, 275, 185, 260, 250, 260	7	254	0.8825
VS-4	1.6	285, 290	2	288	0.9990
VS-4	2.1	220, 270	2	245	0.9063
VS-4	2.25	205, 205, 235, 225, 215, 235, 220, 215, 215, 190	10	216	0.9738
VS-4	2.5	225	1	225	1.0000
VS-4	3.2	280	1	280	1.0000
VS-4	3.5	275	1	275	1.0000
VS-5	0.3	115, 150, 120	3	128	0.9639
VS-5	1.8	255, 250, 270	3	258	0.9890
VS-5	2.0	290, 280, 290, 290, 285	5	287	0.9976
VS-6	1.1	130, 110	2	120	0.9848
VS-6	1.7-1.85	155, 140, 150, 160, 125, 145, 145, 145	8	146	0.9854
VS-6	2.4	140, 155, 165, 130, 130, 125	6	141	0.9680
VS-6	4.5	155, 160	2	158	0.9990
VS-6	5.2	155, 155	2	155	1.0000
VS-7	1.0	280, 275, 270, 330, 335	5	288	0.8803
VS-8	1.0	310	1	310	1.0000
VS-8	1.4	350, 300	2	325	0.9063
VS-8	1.9-2.9	260, 260, 290	3	270	0.9698
VS-8	5.25	apparent: 120	1	120	1.0000
VS-9	0-1.2	apparent: 230, 230	2	230	1.0000
VS-9	1.2-2.0	260	1	260	1.0000
VS-9	2.5-3.0	305	1	305	1.0000
VS-10	n/a	n/a	n/a	n/a	n/a

Appendix B: Key to be Referenced for all Stratigraphic Columns

	Sharp contact		Clast-supported gravel
	Gradational contact		Cross-bedded gravel
	Erosional contact/scour surface		Matrix-supported diamicton
	Massive sand		Silt
	Ripples		Clay
	Ripples with mud drapes		Clay (red)
	Low-angle climbing ripples		Paleocurrent orientation (north towards top of page)
	Low-angle climbing ripples with mud drapes		Rip-up clasts (red clay)
	High-angle climbing ripples		Deformation
	Climbing 3D ripples		Flame structures
	Symmetrical ripples		Load structures
	Symmetrical ripples with fine-grained sand drapes		
	Symmetrical ripples with silt drapes		
	Symmetrical ripples with clay drapes		
	Planar 2D cross-beds		
	Trough 3D cross-beds		
	Horizontal laminations		

Appendix C: Author's Complete Stratigraphic Columns



Figure 39. Photograph of section VS-1. Orange ruler for scale; entire ruler is 30 cm in length.

VS-1
 N44°24.721', W88°00.206'
 Elevation: 244 m
 Date: 09/14/2009

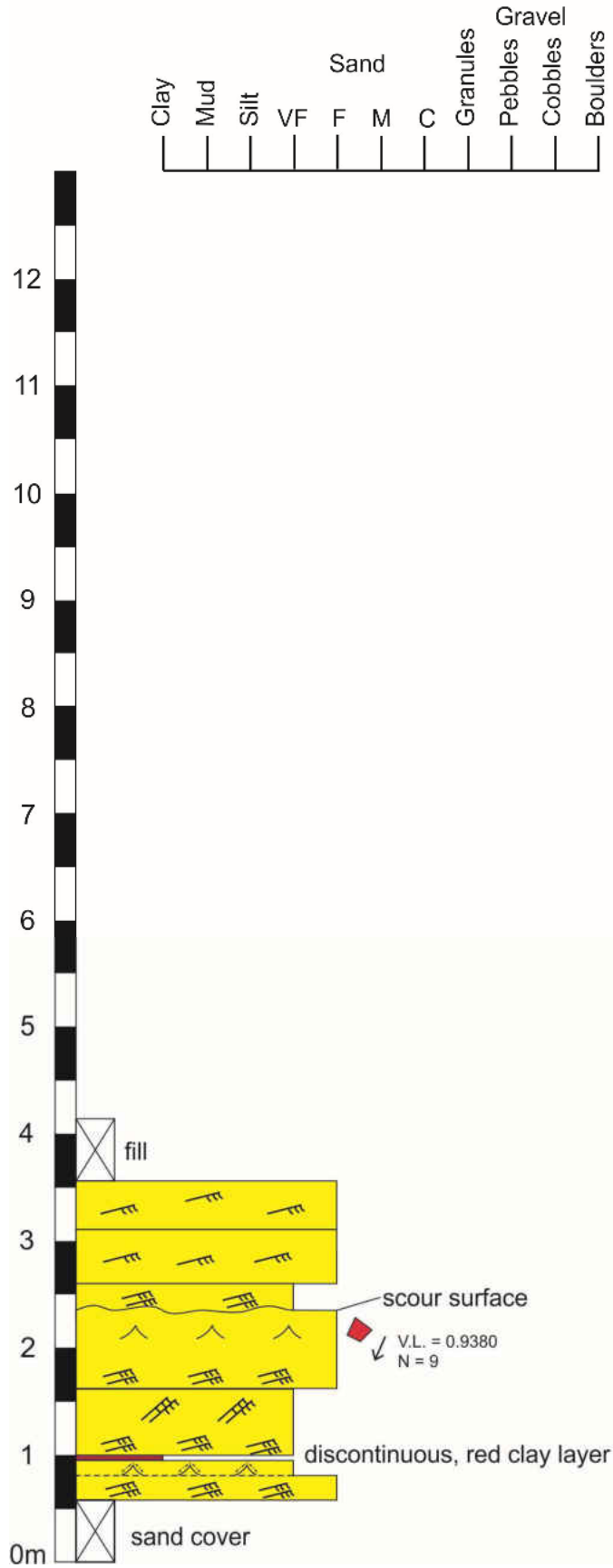




Figure 40. Photograph of section VS-2. Field notebook (7.5 cm in length) for scale.

VS-2
N44°24.719', W88°00.226'
Elevation: 252 m
Date: 09/14/2009

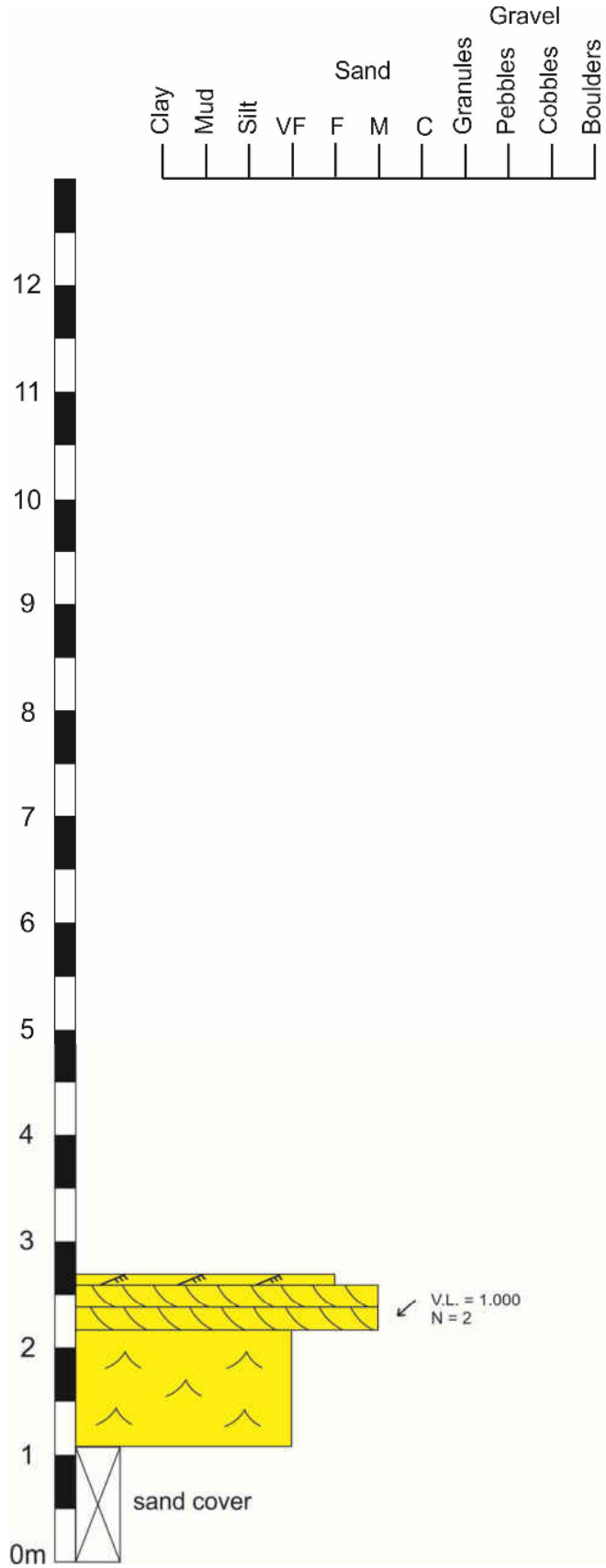
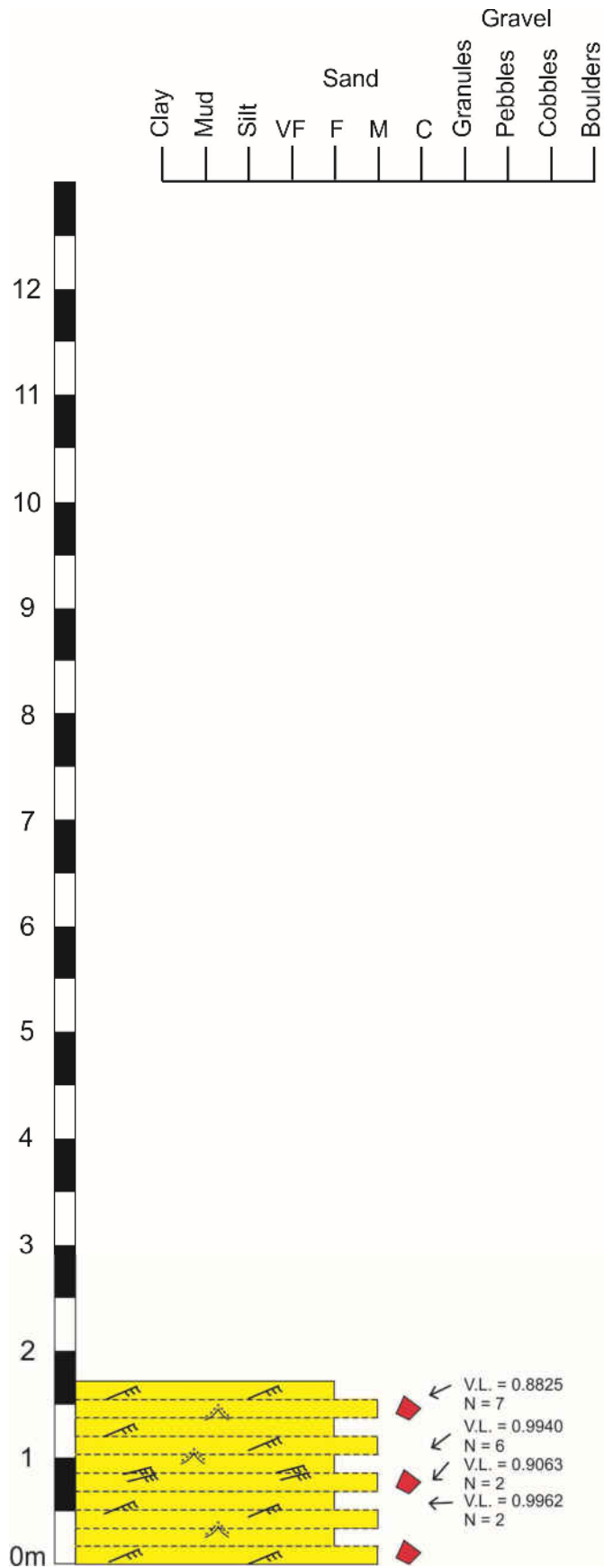




Figure 41. Photograph of section VS-3. Jacob's staff for scale; yellow lines are 10 cm apart.

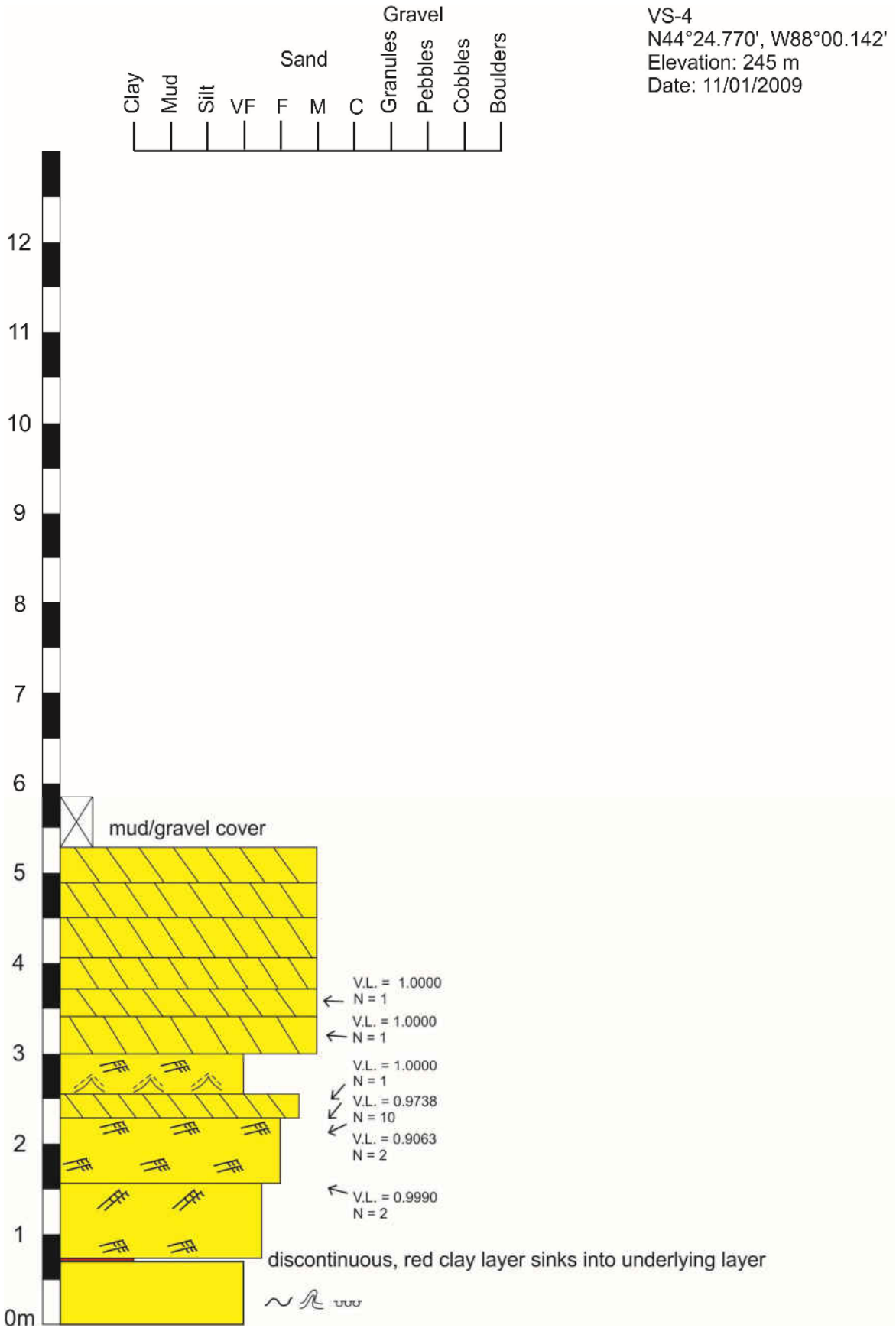


VS-3
 N44°24.734', W88°00.259'
 Elevation: unknown
 Date: 10/25/2009



Figure 42. Photograph of section VS-4. Jacob's staff for scale; staff is approximately 1.5 m in length.

VS-4
 N44°24.770', W88°00.142'
 Elevation: 245 m
 Date: 11/01/2009



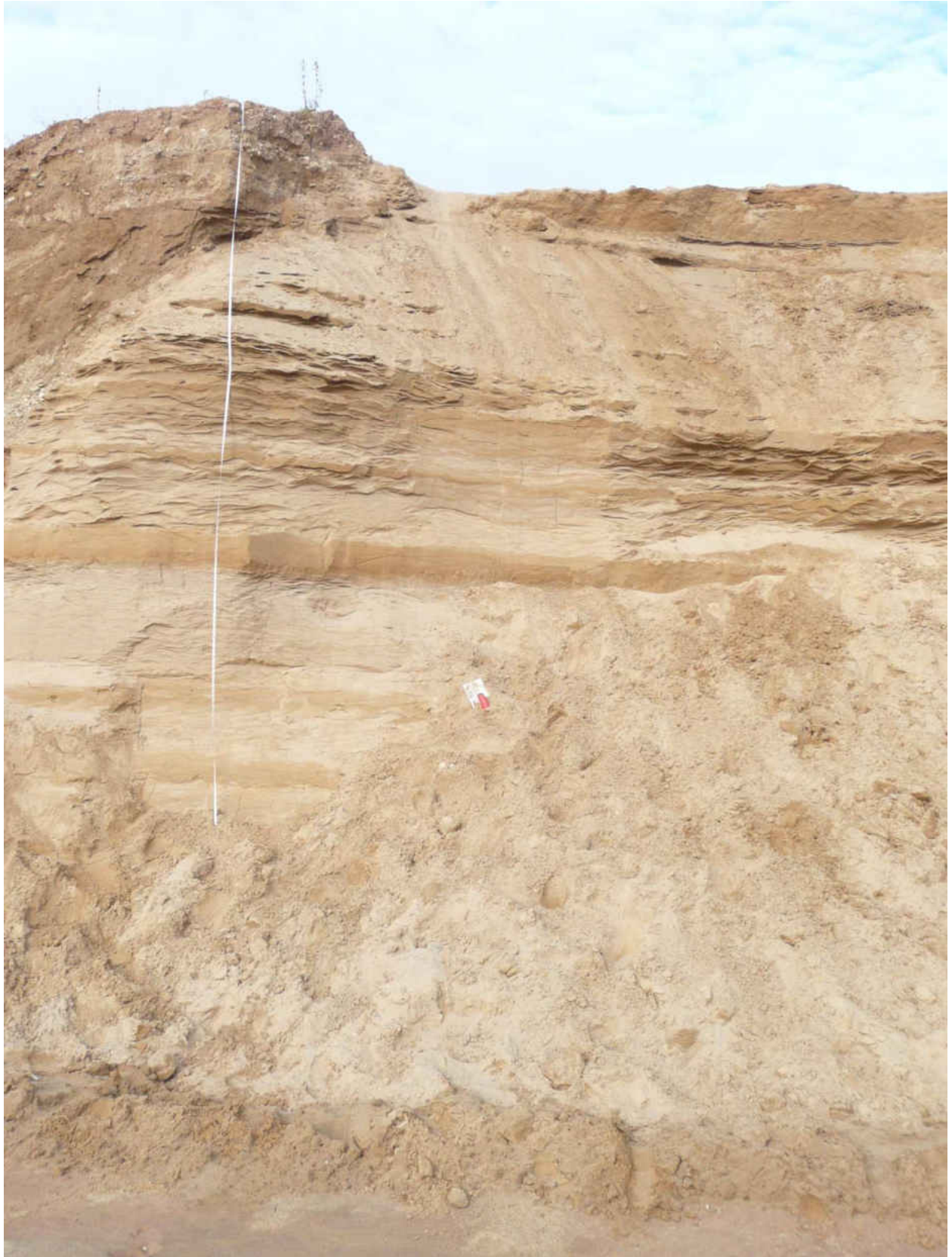


Figure 43. Photograph of section VS-5. Entire section measures 6.0 m in height.

VS-5
 N44°24.782', W88°00.153'
 Elevation: 245 m
 Date: 11/01/2009

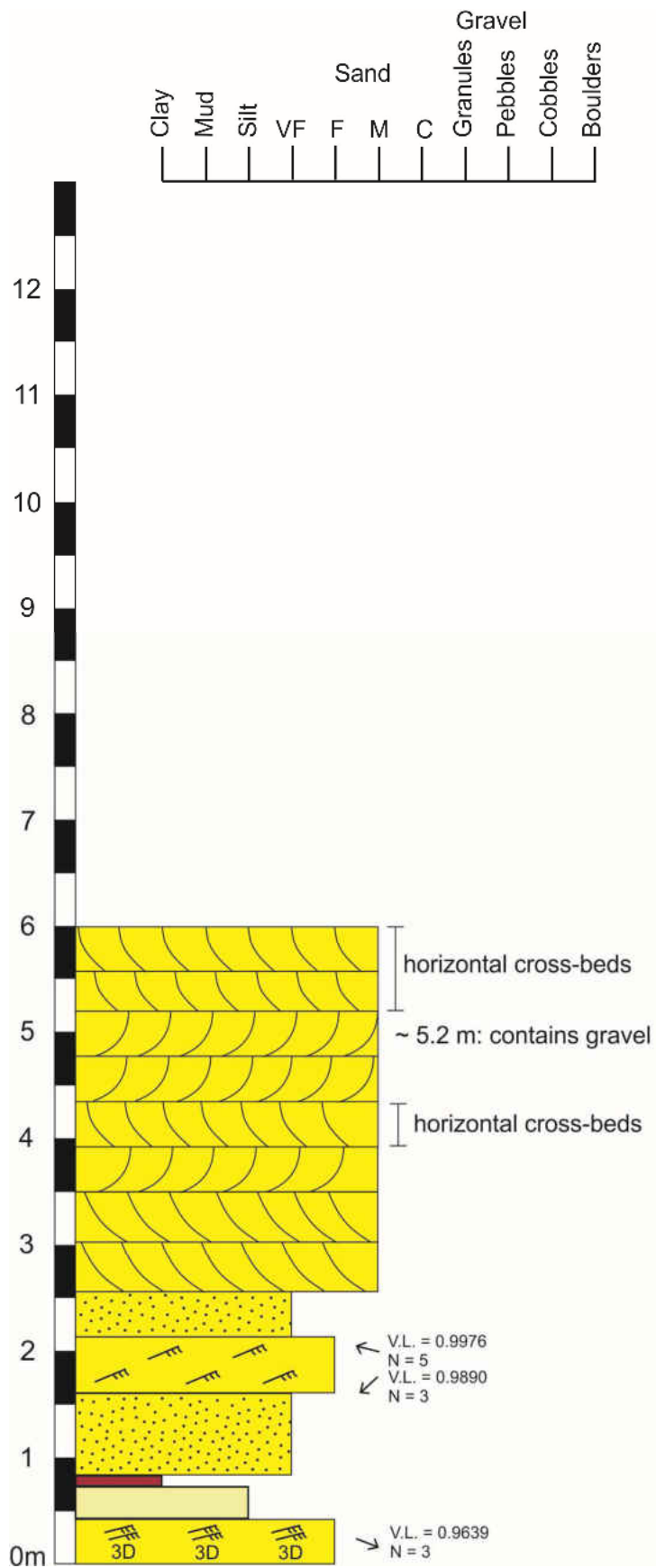
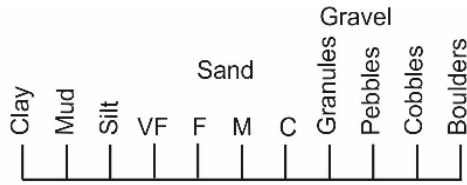




Figure 44. Photograph of section VS-6. Entire section measures 6.0 m in height.



VS-6
 N44°24.805', W88°00.217'
 Elevation: 252 m
 Date: 11/01/2009

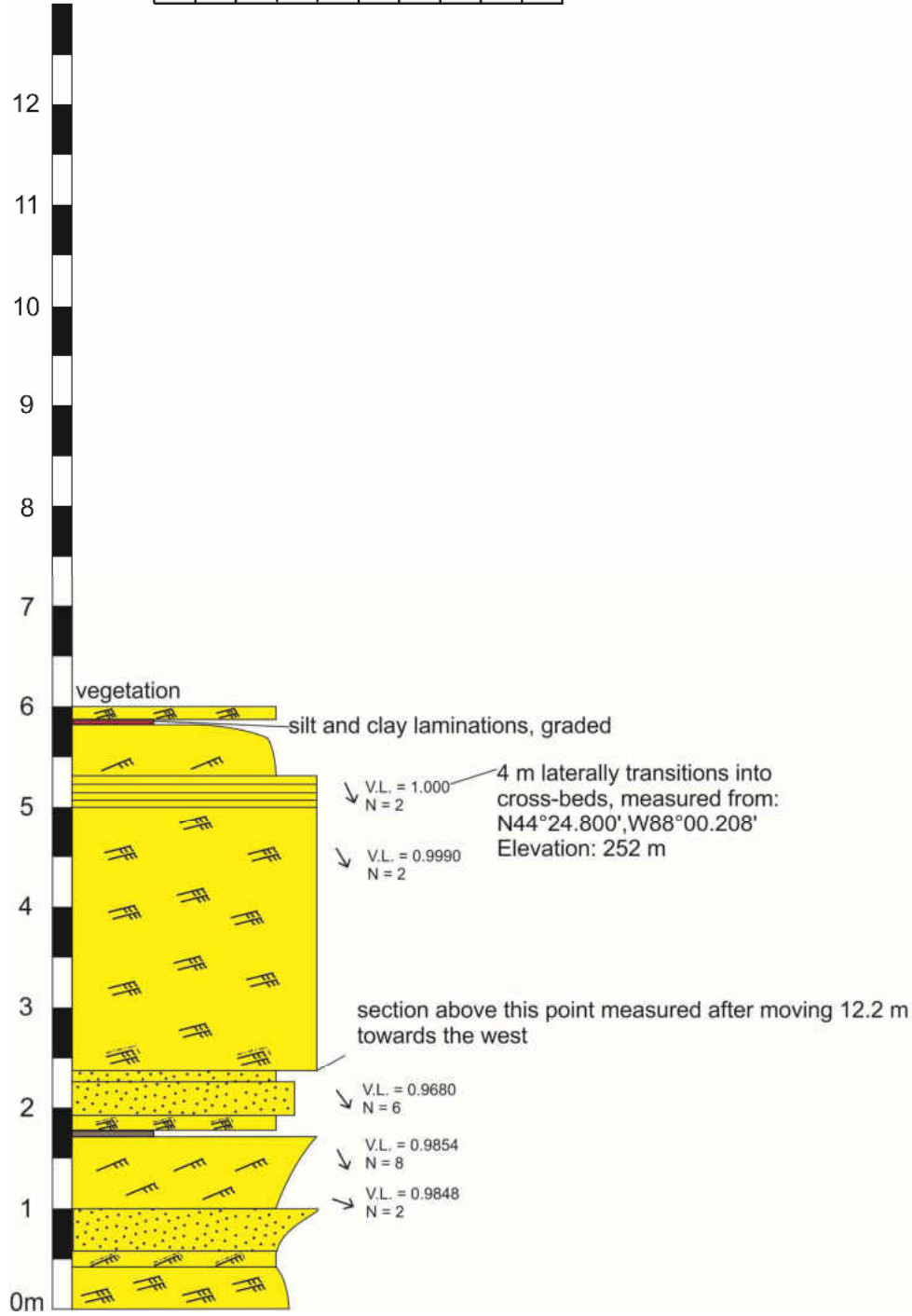




Figure 45. Photograph of section VS-7. Jacob's staff for scale; entire staff is approximately 1.5 m in length.

VS-7
 N44°24.792', W88°00.128'
 Elevation: 261 m
 Date: 11/09/2009

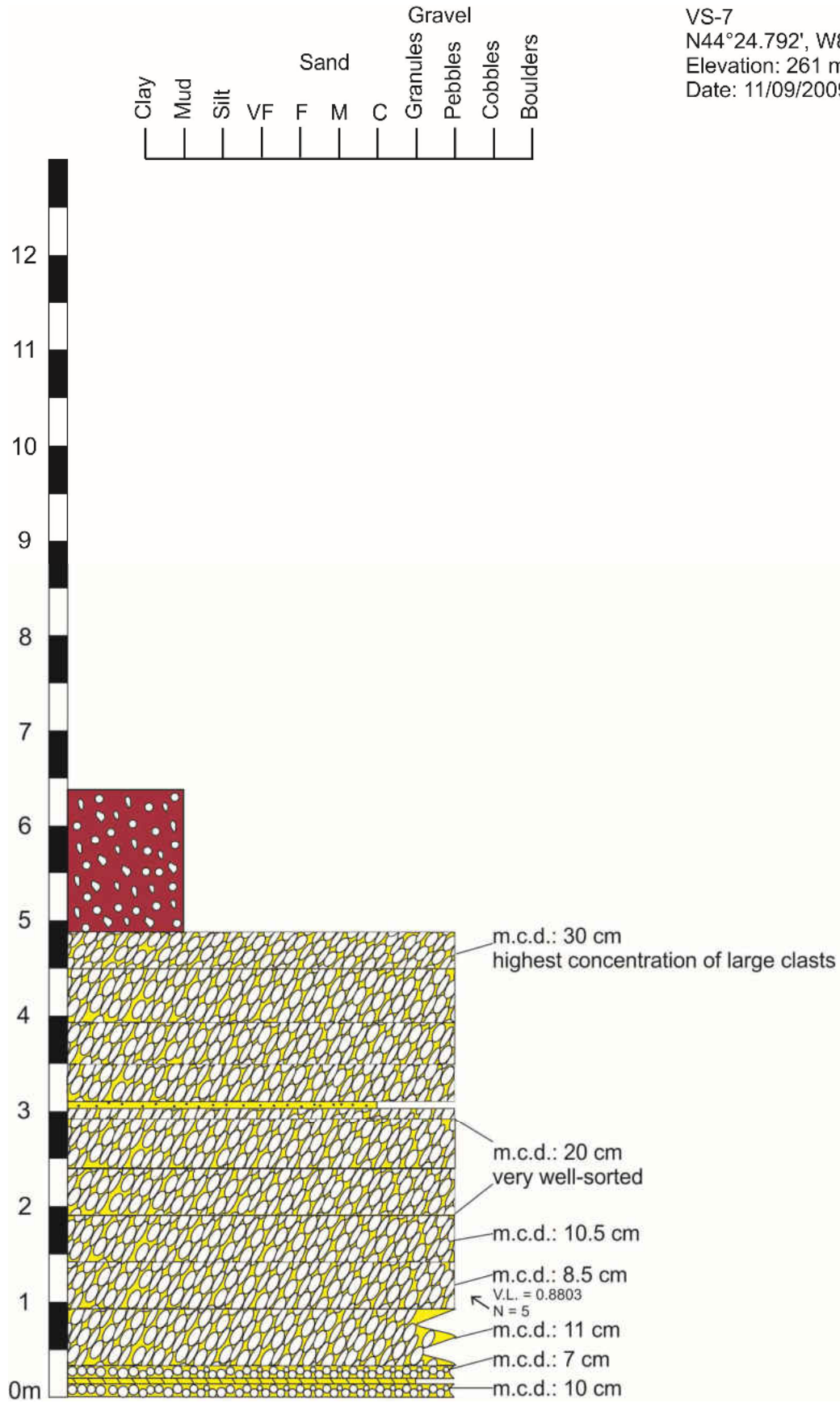




Figure 46. Photograph of section VS-8. Jacob's staff for scale; staff is approximately 1.5 m in length.

VS-8
 N44°24.808', W88°00.142'
 Elevation: 248 m
 Date: 11/09/2009

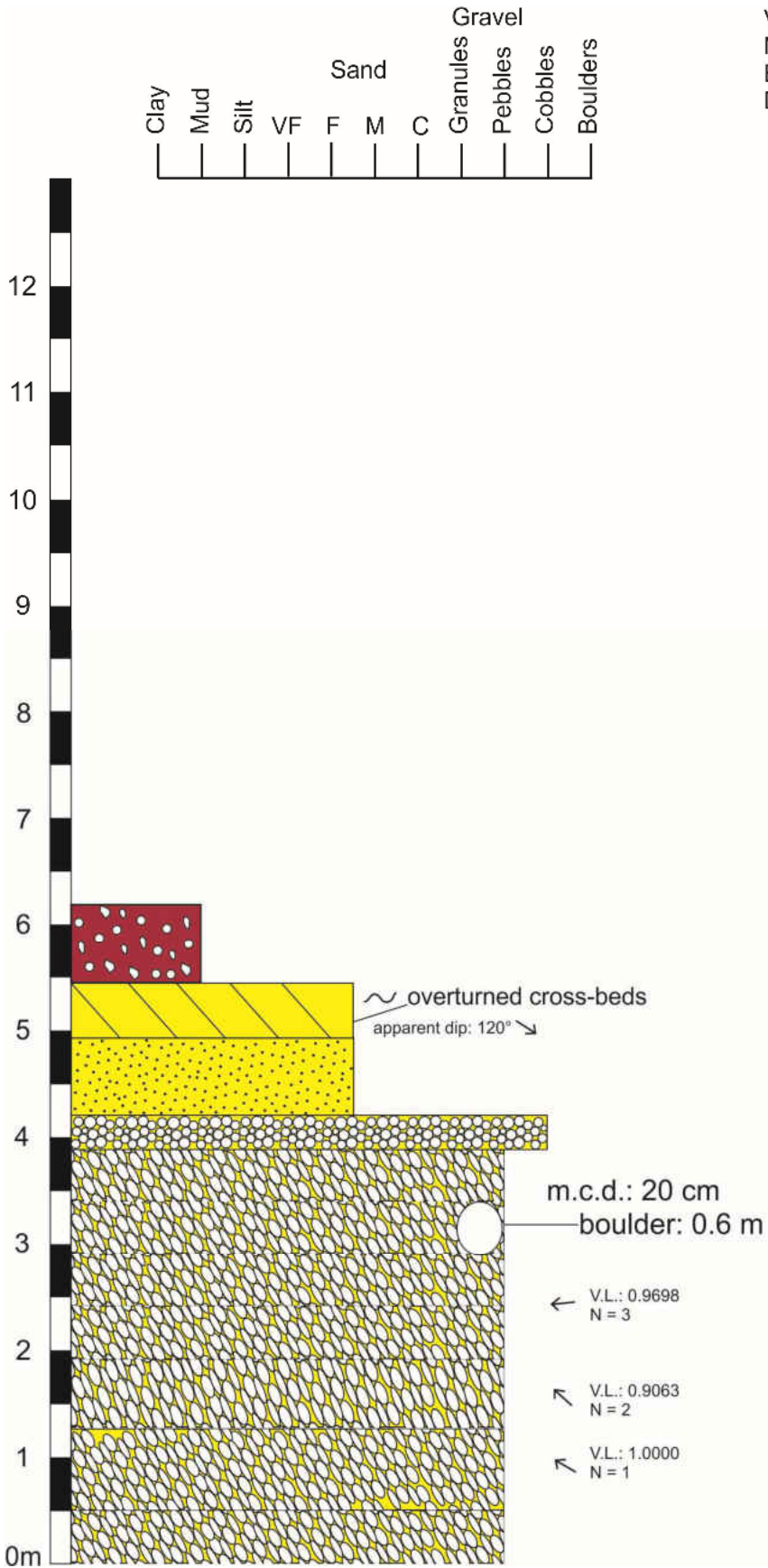
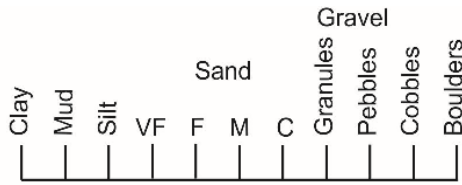




Figure 47. Photograph of section VS-9. Jacob's staff for scale; staff is approximately 1.5 m in length.



VS-9
 N44°24.819', W88°00.188'
 Elevation: 243 m
 Date: 11/09/2009

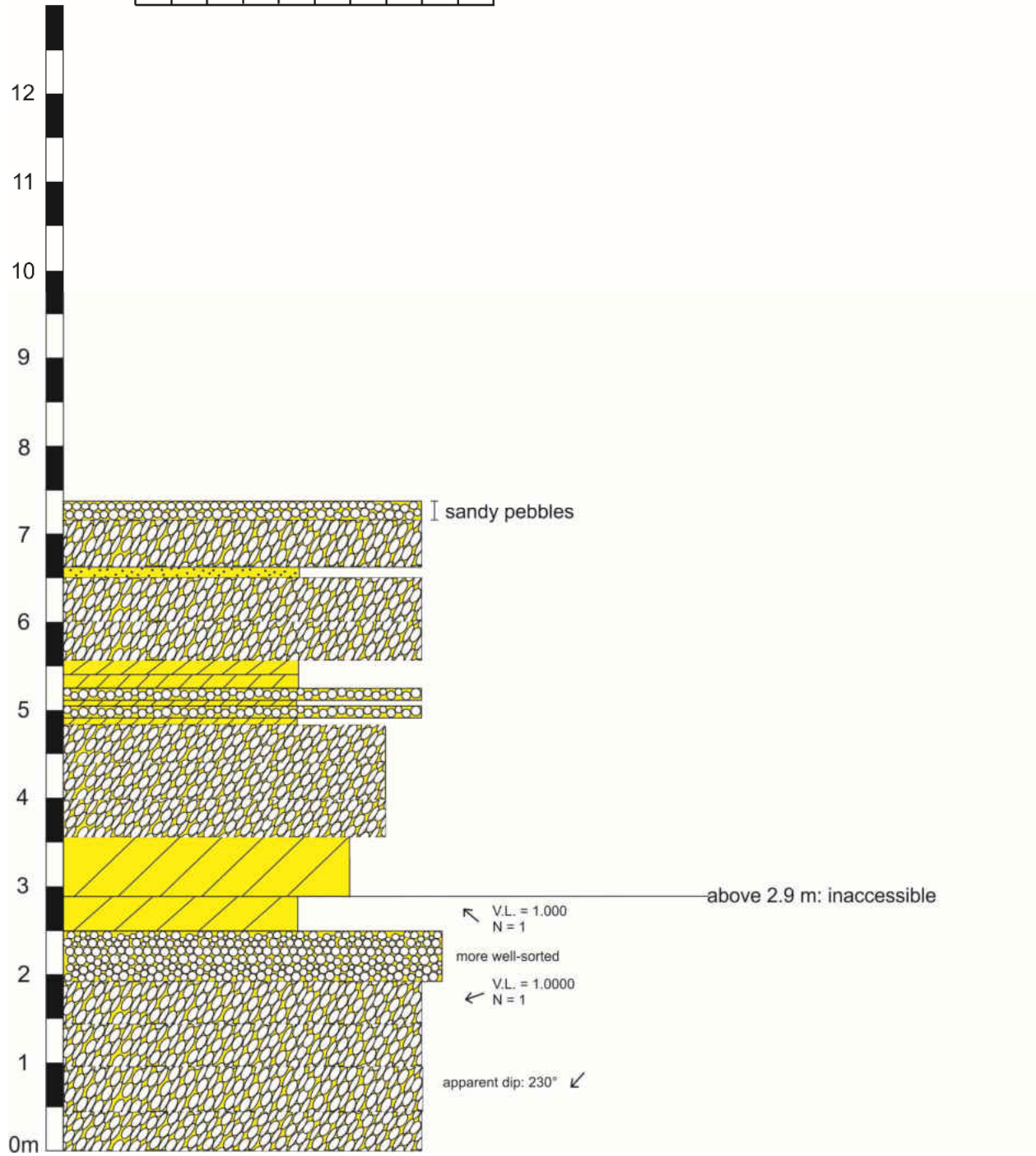
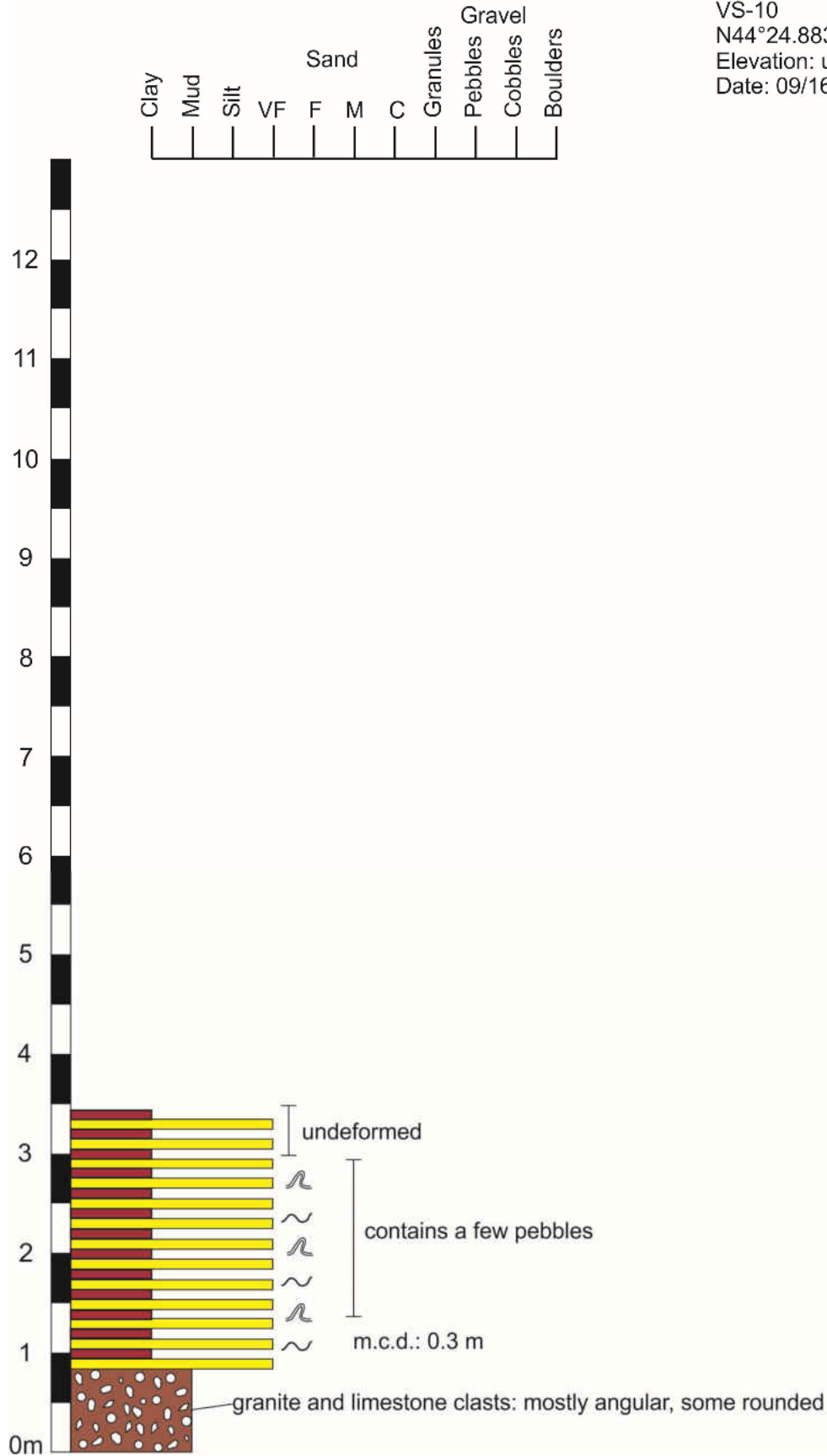




Figure 48. Photograph of section VS-10.

VS-10
 N44°24.883', W88°00.306'
 Elevation: unknown
 Date: 09/16/2011



Appendix D: List of Abbreviations to be used with Stratigraphic Columns

C: coarse

F: fine

M: medium

m.c.d.: maximum clast diameter

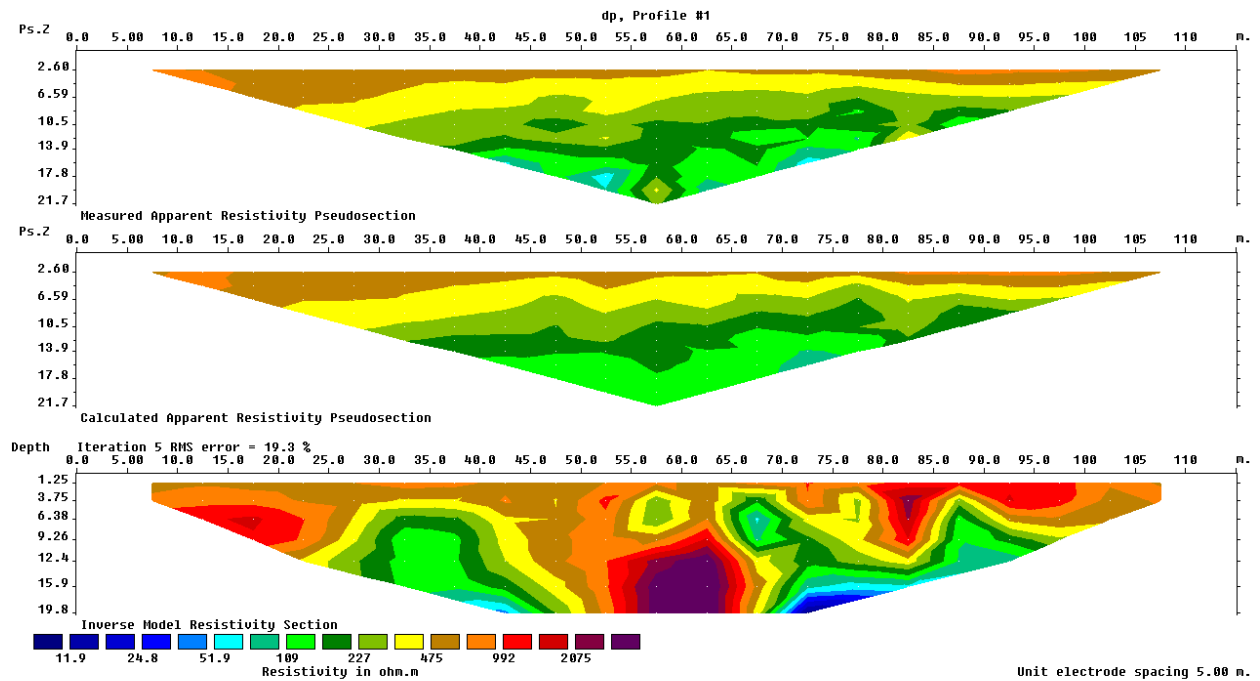
N: number of measurements

VF: very fine

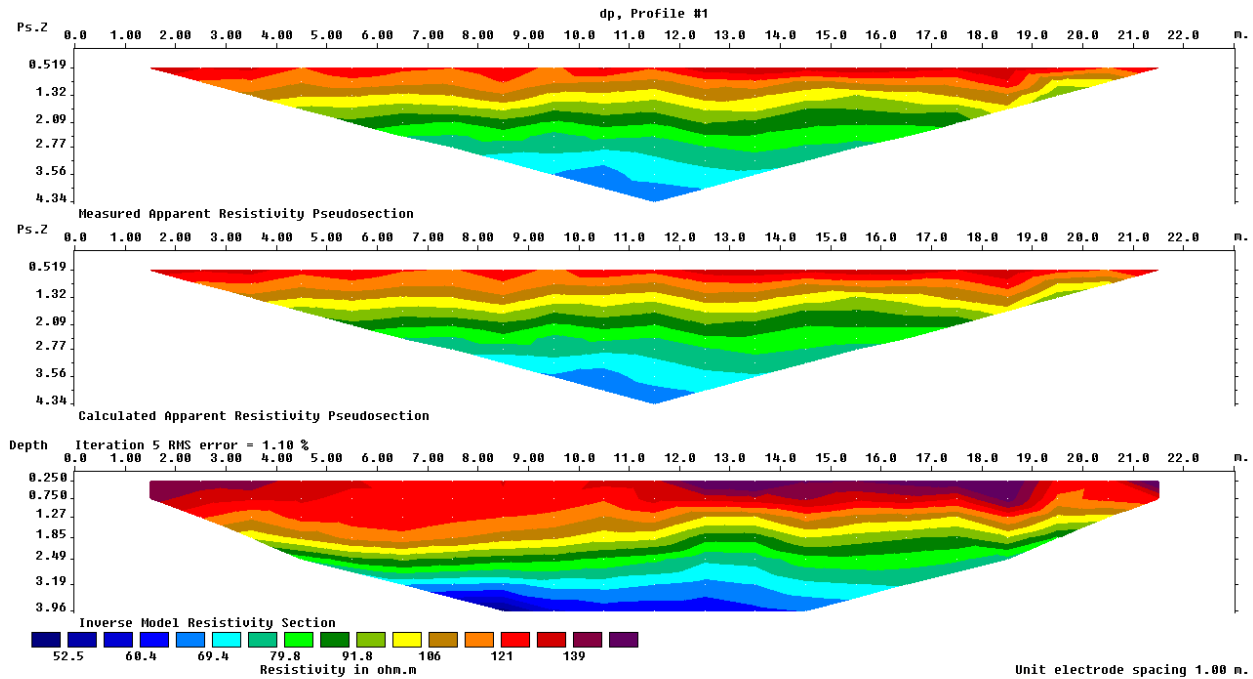
V.L.: vector length; in Stereonet9: "mean length all"

Appendix E: Electrical profile data generated using an ARES Resistivity System

The electrical profile data was generated using an ARES Resistivity System and interpreted using RES2DINV resistivity inversion program. The data collection and processing were done by students at the UW-Milwaukee Geosciences Department as part of the Electrical Methods class in 2010. Two profiles are provided with descriptions available below.



Upper bench area using 24 electrodes spaced at 5 meter intervals.



Base level with spacing between the electrodes of 1 meter.

The GPR data was collected in 2010 using GSSI TerraSIRch SIR System 3000 with a 500 MHz antenna. The equipment was supplied by the Wisconsin Geological and Natural History Survey and instruction on-site was provided by Dr. David Hart of the Wisconsin Geological and Natural History Survey. Data was interpreted using GSSI RADAN software by Geosciences students at the University of Wisconsin – Milwaukee as part of the Electrical Methods course.

Additional details of the data and interpretation, along with uninterpreted DMZ files, are available from Dr. William Kean of the University of Wisconsin – Milwaukee, in the form of student reports from the class.